A COMPREHENSIVE CLIMATOLOGY OF SIGNIFICANT TORNADOES IN THE GREENVILLE-SPARTANBURG, SOUTH CAROLINA COUNTY WARNING AREA (1880-2006)

Justin Lane
NOAA/National Weather Service
Greer, South Carolina

Abstract

A climatology of significant tornadoes (ST) has been developed for the Greenville-Spartanburg, SC (GSP) County Warning Area (CWA). In addition to a time of day/time of year/location climatological analysis, a synoptic climatology has also been developed. This was done to assist operational forecasters in recognizing the "average" synoptic conditions that typically accompany ST occurrence in the GSP CWA. A sounding climatology and sounding parameter climatology was also developed to assist forecasters in assessing the "average" environmental conditions that exist during ST events. The results of this study indicate that ST typically occur in the late afternoon and early evening, and are most common from March through May. ST are most prevalent in the Piedmont region of Upstate South Carolina, northeast Georgia, and southwest North Carolina. Meanwhile, ST are extremely rare in the mountainous areas. The typical ST environment is one in which the GSP CWA is located well within the warm sector of a major mid-latitude cyclone. High pressure is located off the east coast, which may be an important detail, since development of cold air damming is unlikely in such a scenario. Finally, ST environments in the GSP CWA are usually characterized by similar values of wind shear, but much weaker instability in comparison with their Great Plains counterpart.

1. Introduction

Significant tornadoes (ST), defined as those rated F2 to F5 on the Fujita Scale, are rare in the western Carolinas and extreme northeast Georgia in comparison with the Great Plains and the lower Mississippi Valley. However, a recent severe weather climatology by Hart (2005) indicated that the Greer, SC WSR-88D (KGSP) coverage area ranked within the top 30% (39th out of 141) in ST occurrence[1] across the United States. More surprisingly, KGSP ranked in the top 12% (16th) in terms of the average annual probability of occurrence of ST.

---

[1] Tornadoes occurring within a 229 km radius of each radar site were considered in this study. It should be noted that the coverage area of KGSP encompasses a larger area than the Greer, SC County Warning Area ($1.65 \times 10^5 \, km^2$ vs. $5.5 \times 10^4 \, km^2$).

To heighten forecaster awareness of the ST threat, this study will provide a comprehensive climatology of ST for the Greenville-Spartanburg, SC (GSP) County Warning Area (CWA) (Fig. 1). In addition, this study will provide forecasters in the area with a climatological basis for evaluating the ST potential for a given time and day.

The second section of this study consists of an explanation of the various data sources used to create this climatology. Section 3 will stratify the occurrence of ST by time of day, time of year, and county, and present an updated historical tornado track map for the GSP CWA. A discussion of the synoptic characteristics typically associated with ST occurrence in the GSP CWA will be presented in section 4. This analysis will include composite maps of various surface and upper air features associated with ST occurrence. Section 5 presents several composites of reanalysis soundings associated with ST occurrence. Section 6 details the results of a statistical analysis of various parameters yielded by soundings that were constructed from reanalysis data. The paper concludes with a discussion of the results in section 7.

2. Data procedures

The Storm Prediction Center (SPC) storm events database (Kelly at al. 1978), was used in compiling a climatological database for the GSP CWA during the 1950 to 2006 period. This database and the manner in which tornadoes are documented in general have deficiencies that have been addressed in previous studies (e.g., Doswell and Burgess 1988). Due to these deficiencies the "Significant Tornadoes" publication (Grazulis 1993, referred to hereafter as G93) was consulted to cross-check the SPC database. This resulted in the addition of several post-1950 tornadoes to the local database. Since the G93 record for ST begins in 1880, the local database was also expanded to include ST documented in G93 that occurred during the 1880-1949 period. The tornadoes comprising the database are listed in Table 1.

Dates with at least one ST were identified as "ST" days. ST days since 1948 were examined more closely, as this time period coincides with the beginning of the upper air observation program. Sixty ST days were identified after 1948. Days with more than one ST were identified as "ST outbreak days." Thirteen of the 60 days qualified as outbreak days. Six-hourly data from the National Centers for Environmental Prediction - National Center for Atmospheric Research (NCEP-NCAR) reanalysis (Kistler, 2001) were examined for each of the 60 days via the Earth System Research Laboratory's (ESRL) on-line database. Maps of temperature, relative humidity, wind, and geopotential height were examined at the surface, 925 hPa, 850 hPa, 700 hPa, 500 hPa, and 300 hPa levels. In addition, analyses of sea level pressure and specific humidity at the 925 hPa and 850 hPa levels were analyzed. Maps were examined for the latest time period prior to tornado occurrence. The location of major weather features was documented in order to subjectively group ST occurrences into various synoptic categories. Based on this analysis, four categories of "ST days" were identified by the position of the synoptic-scale surface low pressure center near the time of ST occurrence (Fig. 2). The four ST categories identified were: 1) Great Lakes (GRL), 2) Ohio/Tennessee Valley (OTV), 3) Eastern Great Plains (EPL), and 4) Southeast Tropical Cyclone (TCY).

To describe the "average" synoptic scale conditions that accompany a ST event across the GSP CWA, composite maps of the above parameters were developed for each of the four ST categories using the compositing tool on the ESRL website (http://www.cdc.noaa.gov/Composites/_Hour/), Twenty-one days were categorized as GRL events. Sixteen days were used to develop the OTV composite. Seven days were identified as EPL events. Six days were used in developing the TCY composites. On 10 of the ST days, there were no significant areas of low pressure, or the position of the low did not fit any of the four categories. Composite maps of ST outbreak days were also developed.

In addition to the composite maps, raw reanalysis data of the above fields were examined. For each outbreak, the values of these parameters were documented at the two grid points nearest the GSP CWA (35° N, 82.5^o W; 35.0^o N, 80.0^o W). Values of air temperature, relative humidity, u and v component of the wind, and geopotential height at the surface, 925 hPa, 850 hPa, 700 hPa, 600 hPa, 500 hPa, 400 hPa, and 300 hPa, 250 hPa, 200 hPa, and 150 hPa levels were documented for each day at the latest time prior to tornado occurrence. From these parameters, the dewpoint temperature, the 700 hPa to 500 hPa lapse rate, and the magnitude and direction of the wind vector were calculated. The bulk wind shear in the surface to 500 hPa layer was also calculated to serve as a proxy to 0-6 km bulk shear.

From the raw reanalysis data, two soundings were constructed for each of the 60 days using Environmental Research Service's Rawinsonde Observation (RAOB) software. The sounding that was deemed most representative of the tornadic environment was selected for further analysis. In the majority of cases, this was the sounding nearest the location of the tornado event(s). From these soundings, values of surface-based Convective Available Potential Energy (CAPE) were documented through the entire depth of the sounding and in the 0-3 km layer. In addition, Storm Relative Helicity (SRH) in the 0-3 km and 0-1 km layers was documented. Finally, the values of Bulk Richardson Number (BRN) and the Energy Helicity Index (EHI) were recorded. From this collection of data, the median, average, 1st and 3rd quartile values were calculated for each of the above fields, as well as for values of 700 hPa to 500 hPa lapse rate and surface to 500 hPa bulk shear. This statistical data is presented in box-and-whisker plots in Section 5.

Once the sounding data were documented, composite soundings were constructed using the RAOB software for each of the four ST synoptic categories. Composite soundings were also developed for ST outbreak days and for all 60 ST days.

3. Time and location climatology

a. Location

Paths of each of the 176 ST that have affected the CWA since 1880 are detailed in Fig. 3. ST occurrence is most common across the Piedmont and foothills region of Upstate South Carolina and northeast Georgia, and the southern Piedmont of North Carolina.

Geographically, this region represents approximately 50% of the GSP CWA. However, 153 (or 86%) of the ST that have affected the CWA began in or otherwise affected this region. This distribution can largely be attributed to the rugged terrain over far western North Carolina (Fig. 1). Only three ST have been reported in this mountainous region since 1880. In fact, it appears that the terrain not only plays a role in the paucity of tornadoes within the mountains themselves, but also has an affect on ST occurrence immediately east (downstream) of the mountains. ST are much less common across the foothills and northwest Piedmont of North Carolina than they are further south. In examining Fig. 3, one can see that tornadic thunderstorms moving into roughly the southern half of the CWA would most likely originate in central Georgia. Such thunderstorms would interact with little or no complex terrain before moving into the GSP CWA. However, thunderstorms moving into the foothills and northwest Piedmont of North Carolina would most likely originate in the complex terrain of the southern Appalachians. Recent climatological evidence for this evolution is shown by Parker and Ahijevych (2007). Thunderstorms are much less likely to become tornadic over the foothills and northwest Piedmont than in locations further south (Fig. 3). However, it should be noted that in some cases, the mountains may indirectly promote ST development through establishment of a lee trough. Lee troughing often provides a low-level focus for initiation of deep convection over the Piedmont during the warm-season (Weisman 1990).

Figure 3 indicates the area most affected by ST are in locations from Anderson to Greenville and Spartanburg in South Carolina, east to the Charlotte metro area in North Carolina. This area includes the most populous counties in North Carolina (Mecklenburg) and in South Carolina (Greenville). Given the documented impact of population on the United States tornado climatology (e.g. Schaefer at al. 1993) there can be little doubt that the GSP ST distribution is at least partially influenced by population.

Figure 3 reveals that F3 and F4 tornadoes are most common across the lower elevations of Upstate South Carolina and northeast Georgia, and the southern Piedmont of North Carolina. Seventeen of the 19 F3 tornadoes and seven of the eight F4 tornadoes that have affected the CWA touched down in or affected this area. There have been no recorded instances of F5 tornadoes in the GSP CWA.

b. Time of day

The chart in Fig. 4 illustrates the diurnal distribution of ST in the GSP CWA. The local time conversion is LT(EST) = UTC − 5h. There is a minimum of tornadic activity (3.5% of total occurrence) in the pre-dawn hours, with a gradual increase in the mid and late morning (5.8%). There is a rapid increase in tornado occurrence from the late morning to the early and mid afternoon (22.2%). Occurrence continues to increase sharply, with peak tornado time being the late afternoon and early evening, during which 46.2% of all ST occur. Occurrence decreases dramatically during the mid-to-late evening (14.0%) and continues decreasing during the overnight hours (8.8%).

c. Time of year

Figure 5 is a graph representing the monthly distribution of ST occurrence in the GSP CWA. The monthly climatology is rather typical of the overall tornado climatology across the conterminous United States. There is a lull in tornado activity in December and January, with only 5.1% of ST occurring in these months. ST incidents begin to increase rather sharply in February, during which 9.0% of all ST occur. Peak ST season is March through May, with a fairly even distribution across the three months. These months contain 62.9% of all ST occurrences. ST occurrence decreases dramatically in June and July, with only 6.2% of ST events occurring during this time. There is a slight increase in ST activity during August and September (9.6% of occurrences.) This can be attributed to increasing tropical cyclone activity. Another lull in ST activity is experienced in October. ST activity briefly increases again in November before settling into the early winter lull.

4. Composite analyses

For many years, pattern recognition has been an essential component in forecasting the potential for severe deep moist convection and tornadoes (Doswell et al. 1993). One technique that has been utilized to facilitate pattern recognition is use of the "composite chart" (Miller 1972; Barnes and Newton 1983). Figure 6 is a composite chart representing the location of various synoptic scale features with respect to an outbreak of severe and/or tornadic thunderstorms. The hatched area in the figure represents the location most favorable for development of severe convection, where wind shear and instability are maximized in the region southeast of the surface cyclone. In this region warm, moist air in the lower levels results in positive CAPE, while the intersection of the lower and upper jets provides a clockwise-turning hodograph, which contributes to large values of SRH. This is considered the "textbook" synoptic pattern conducive to outbreaks of severe weather. However, it is primarily based on Great Plains cases. The GSP CWA ST composite results will be compared to this "textbook" synoptic pattern to elicit regional differences.

a. Great Lakes (GRL) composite

The composite of sea level pressure for the GRL category is presented in Fig. 7a. An area of surface low pressure of around 1000 hPa is located over south-central Michigan. A trough, possibly indicating the position of the surface cold front, extends from the low pressure area across the western Ohio valley into the lower Mississippi valley and into the western Gulf of Mexico.

A southwesterly low level jet of greater than 15 m s^{-1} extends from the central Gulf of Mexico coast, through the Tennessee Valley and the Carolinas, into extreme southern New York (Fig. 7c). A maximum in wind speed of 18 m s^{-1} is present over the southern and central Appalachians. An influx of moisture from the eastern Gulf of Mexico is evident at 850 hPa (Fig. 7b), with a maximum in low level moisture over the southern Appalachians.

A 500 hPa trough, with a slight negative tilt is evident across the Mississippi Valley (Fig. 7d). The composite of 300 hPa wind (Fig. 7e) reveals a large wind maximum with speeds of around 35 m s^{-1} extending from the lower Mississippi Valley across the Tennessee and Ohio Valleys into the eastern Great Lakes.

Comparison of the features from the GRL composite analyses to the composite chart in Fig. 6 reveals that each features a vigorous extratropical cyclone with a strong low level wind maximum. However, the low level jet in Fig. 7c is displaced 600 to 700 km east of the surface low and associated cold front. This is opposed to the distance of 100 to 200 km that is suggested in Fig. 6. As a result, the GSP CWA is much further south and east of the surface low when compared with the "outbreak area" outlined in Fig. 6. In addition, the upper level jet axis (Fig. 7e) does not cross the low level jet axis (Fig 7c) as is shown in Fig. 3. The axes of the two jets are actually parallel in the GRL case, with the 300 hPa jet axis located 200 to 300 km west of the 850 hPa jet.

b. Ohio/Tennessee Valley (OTV) composite

The composite of sea level pressure for the OTV scenario (Fig. 8a) reveals an area of low pressure (~1003 mb) over south central Kentucky. A trough, likely delineating the position of the surface cold front, extends from the low through the Tennessee Valley and across the central Gulf Coast. Another trough, possibly representing the warm front, extends east of the low across Virginia and off the mid-Atlantic coast.

The composite analysis of 850 hPa wind (Fig. 8c) indicates a southwesterly jet with wind speeds of 15 m s^{-1} or greater extends from the central Gulf Coast to the vicinity of the Virginia/Kentucky border. A wind speed maximum of around 19 m s^{-1} is observed over central Georgia. The composite of specific humidity at 850 hPa in Fig. 8b indicates a maximum in low level moisture extending from the eastern Gulf of Mexico through the Carolinas and into the central Appalachians.

A neutrally tilted trough in the 500 hPa height field (Fig. 8d) is observed across the Mississippi Valley. This trough position is very similar to that in Fig. 7d. The composite analysis of 300 hPa wind (Fig. 8e) indicates dual jet maxima across the eastern United States. The axis of one jet max (> 35 m s^{-1}) extends from southeast Texas into the Tennessee Valley and the southern Appalachians. Peak wind speeds of 38 m s^{-1} are observed from central Alabama into northwest Georgia. A second jet maximum is evident from the eastern Great Lakes into New England.

Comparison of Figs. 6 and 8 indicates that the axis of the low level jet in the OTV composite is 300 km to 400 km southeast of the surface cyclone and cold front, approximately twice the distance suggested in Fig. 6. As is the case with the GRL category, the axes of the upper and low level wind maxima do not cross, but rather are parallel and separated by a distance of 300 to 400 km.

c. Eastern Plains (EPL) composite

The composite analysis of sea level pressure for the EPL category (Fig. 9a) reveals an area of surface low pressure, with a minimum pressure of around 995 hPa located over eastern Iowa. A surface trough or cold front extends from the surface cyclone across the Missouri into eastern Oklahoma and central Texas.

The composite of 850 hPa wind (Fig. 9c) reveals a broad area of wind speed greater than 15 m s^{-1} covering much of the eastern United States. However, the main axis of the low level jet extends from the Arkansas and east Texas into the Ohio Valley and lower Great Lakes. The low level wind maximum (~20 m s^{-1}) is located over western Kentucky and extreme southern Illinois. A southerly fetch off the Gulf of Mexico is resulting in enhanced low level moisture across much of the southeast and the eastern Ohio Valley (Fig. 9b). The maximum in 850 hPa moisture is located over southwest Virginia.

The composite analysis of 500 hPa geopotential height (Fig. 9d) indicates a closed mid-level circulation over western Iowa and southern Minnesota. A trough with a negative tilt extends from the low pressure center across Missouri into the lower Mississippi Valley. An axis of 300 hPa winds greater than 35 m s^{-1} (Fig. 9e) extends from northeast Texas through the lower Mississippi Valley and into the Ohio Valley. A maximum in 300 hPa wind speed of around 40 m s^{-1} is observed over western Kentucky.

Comparison of the EPL composite analyses with the composite chart in Fig. 6 reveals that the upper and lower jet axes intersect over western Kentucky, although not at the sharp angle indicated in Fig. 6. One significant difference between Fig. 6 and the ERL composite analysis is that the GSP CWA is several hundred kilometers further southeast with respect to the surface cyclone than the "outbreak area" outlined in Fig. 6. However, it should be noted that many of these cases were associated with significant outbreaks of severe weather across the Tennesse, Ohio, and Mississippi Valleys. The GSP CWA was located on the eastern periphery of these outbreak areas.

d. Tropical Cyclone (TCY) composite

The composite analysis of sea level pressure for the TCY category is shown in Fig. 10a. The center of a remnant tropical cyclone (minimum surface pressure of around 1005 hPa) is indicated near the Alabama/Georgia border. This places the GSP CWA within the right front quadrant of the cyclone. This is consistent with past observations of tornado outbreaks associated with landfalling tropical cyclones (Novlan and Gray 1974; McCaul 1991). In all six TCY cases, the cyclone made landfall on the coast of the Gulf of Mexico.

An analysis of 850 hPa wind (Fig. 10c) reveals a low-level jet of greater than 10 m s^{-1} east of the cyclone center, extending from the north central Gulf of Mexico to the Georgia coast though South Carolina. A maximum in wind speed of greater than 12 m s^{-1} is located over the northern Florida peninsula. Figure 10b is the composite analysis of

specific humidity at 850 hPa for the TCY scenario. A maximum in low level moisture extends from Alabama and Georgia into the western Carolinas.

The composite of 500 hPa features the closed circulation of a remnant tropical cyclone over northern Alabama (Fig. 10d). The 300 hPa wind composite in Fig. 10e indicates a rather typical late summer pattern, with the main axis of the polar jet confined to northern portions of the United States. Upper level wind speeds across the Southeast are rather weak, generally less than 15 m s^{-1}.

Considering the time of year that coincides with peak tropical cyclone activity in the North Atlantic basin, it is not surprising that the TCY scenario is the ST category that is most dissimilar to the "classic" synoptic outbreak pattern as depicted in Fig. 6. With the axis of the polar jet located well north of the GSP CWA, upper level winds are quite weak, and there is an absence of the vigorous mid-level trough that is present in the other categories. However, low level shear and instability are present.

e. Comparison of the four ST categories

The GRL and OTV categories are similar in terms of the placement and intensity of significant synoptic features, including the intensity of the surface low, jet configurations, and position of the 500 hPa trough axis. The only significant difference is that the surface low in the OTV category is approximately 200 km from the CWA, as opposed to 750 km for the GRL category.

The EPL category features the strongest, most well-developed cyclone among the four categories. The minimum central pressure is five to ten hPa lower than in the other categories. However, the surface low is much farther west of the region of interest than in other categories. The EPL bears some similarities to the "classic" severe weather outbreak pattern depicted in Fig. 6, as the low level and upper level jet axes are in close proximity, and actually intersect over a small area in the western Ohio Valley. Five of the seven ST days that were identified as EPL cases also qualified as outbreak days. The only other ST category that contained as many or more outbreak cases was GRL (also with five). The other categories contained no more than one outbreak case.

One of the more important similarities of the GRL, OTV, and EPL scenarios is that all three composites feature 850 hPa wind speeds of 16 m s^{-1} to 20 m s^{-1} over the GSP CWA. Also, the synoptic scale low level wind maximum coincides with a maximum in low level moisture over the GSP CWA. This is especially true in the OTV and GRL scenarios, which are the most representative categories. Obviously, this scenario enhances the potential for strong low level wind shear to coexist with areas of convective instability.

The position of the surface low in the GRL and EPL categories is well north of the region of interest than what is suggested by the "outbreak area" in Fig. 6. This may be an important detail related to ST occurrence in the GSP CWA. When strong extra-tropical cyclones track over or south of the GSP CWA, most of the western Carolinas and

northeast Georgia remain within the cold sector, with cold air damming developing north of the warm front along the eastern slopes of the Appalachians (e.g. Bell and Bosart 1988). Once this very stable airmass becomes established, it often does not completely erode until after cold frontal passage (Lackmann and Stanton, 2004). This prevents development of surface-based convection during these events, thereby eliminating the tornado threat. However, in each composite analysis, the GSP CWA is located well within the warm sector of the extratropical cyclone. Examination of the analyses of sea level pressure from these composites reveals high pressure that is located well off the Atlantic Coast, minimizing the potential for cold air damming (Bailey et al. 2003).

Another significant point that can be inferred from the composite analyses is the fact that, in many ST events, the surface cold front apparently plays little or no role in initiating severe, tornadic convection. For the three non-tropical categories, the position of the cold front in the 0-6 hour window prior to ST occurrence ranges from ~100 km (in the OTV category) to ~1000 km (in the EPL category) west of the region. In the most common category (GRL), the cold front is ~500 km west of the GSP CWA. This suggests that deep convection producing STs is more common in the warm advection pattern ahead of the surface cold front, where mesoscale processes may initiate discrete, cellular convection well in advance of the deep, linear forcing associated with the cold front.

The ST outbreak composite bears a strong resemblance to the GRL composite analyses. There is a vigorous, migrant trough located over the Great Plains (Fig. 11d) and an associated surface low near Lake Michigan (Fig. 11a). The low level wind maximum is positioned over the GSP CWA (Fig. 11c). There is also an area of enhanced low level moisture extending across the GSP CWA (Fig. 11c). Meanwhile, the axis of the upper level jet is west of the low level jet axis, and there is no intersection between these air streams (c.f., Fig. 11c,e). Thus, it may be difficult to discriminate between 1 ST or an ST outbreak.

5. Composite soundings

A composite sounding was developed for each ST category by averaging the soundings described in section 2. Only mandatory levels were used in development of the proximity soundings. The absence of intermediate data may diminish the accuracy of the sounding parameters. However, high resolution reanalysis data were not available for all 60 days. Not surprisingly, the parameter values yielded by the composite soundings are in some instances significantly different than the averages from the individual soundings. Table 2 details the mean and median values produced by the individual soundings vs. the values yielded by the composite soundings.

Figure 12 is the composite sounding for the GRL category. A veering wind profile is indicated with approximately 23.2 m s^{-1} of deep layer (0-6 km) shear. This is slightly less than the mean deep layer shear magnitude (24.5 m s^{-1}) found by Thompson et al. (2003; hereafter referred to as T03) to be associated with significant supercell tornadoes. Storm relative helicity (SRH) in the 0-1 km (0-3 km) layer is 118 m^2 s^{-2} (205 m^2 s^{-2}). This is weaker than the mean value of 0-1 km and 0-3 km SRH associated with STs (165 m^2 s^{-2}

9

and 223 m^2 s^{-2}, respectively) in T03. Instability parameters indicate surface-based Convective Available Potential Energy (sbCAPE) of 827 J kg^{-1}. This is much less than the mean value of CAPE[2] of 2152 J kg^{-1} found by T03 to be associated with STs. However, CAPE in the 0-3 km layer is 124 J kg^{-1}. This is higher than the mean value of 63 J kg^{-1} found by Rasmussen (2003; hereafter referred to as R03) to be associated with STs. The 0-2 km Energy Helicity Index (EHI) in the sounding is 0.9. This value is near the lower threshold of EHI (1.0) utilized by operational forecasters in assessing the potential for supercells (Rasmussen and Blanchard, 1998).

The composite sounding for the OTV category is shown in Fig. 13. The wind profile is very similar to the GRL category. There is 24.7 m s^{-1} of deep layer shear, which is almost identical to the mean value associated with STs in T03. SRH in the 0-1 km layer is 105 m^2 s^{-2}, which is weaker than the values yielded by the GRL sounding, and weaker than the mean value in T03. SRH in the 0-3 km layer is 206 m^2 s^{-2}. This is similar to the value yielded by the GRL composite sounding and less than the mean value in T03. As is the case in the GRL sounding, sbCAPE in the OTV sounding is quite low at 650 J kg^{-1}. Although CAPE in the 0-3 km layer is a respectable 71 J kg^{-1}. The 0-2 km EHI in the sounding is only 0.7.

The composite sounding for the EPL category is presented in Fig. 14. A strongly veering wind profile is indicated, with deep layer shear of 24.2 m s^{-1}. SRH in the 0-1 km layer is 142 m^2 s^{-2} while the 0-3 km SRH is 231 m^2 s^{-2}. These values are the highest among the four composites. This is largely due to the backed surface flow. Owing to steeper mid-level lapse rates, the EPL sounding contains higher sbCAPE (901 J kg^{-1}) than the GRL or OTV composites. However, a lower surface dewpoint is yielding CAPE in the 0-3 km layer of only 57 J kg^{-1}. The sounding produces an EHI of 1.2. This is the largest value of EHI among the four composite soundings, suggesting that the EPL sounding provides the most favorable combination of shear and instability for tornadic thunderstorms.

A composite sounding for the TCY case is shown in Fig. 15. As in the other composite soundings, a strongly veering wind profile is indicated. However, the profile is almost entirely contained within the upper left quadrant of the hodograph, as opposed to the profiles from the other soundings, which are mostly in the upper right quadrant. The flow is also considerably weaker than in the other composite soundings, particularly in the mid and upper levels of the sounding. This results in deep layer shear of only 14.1 m s^{-1}. Despite the weaker flow, the sounding yields SRH of 76 m^2 s^{-2} in the 0-1 km layer while the 0-3 km SRH is 141 m^2 s^{-2}. It should be noted that the shear parameters in the TCY sounding are much weaker than those yielded by McCaul's (1991) composite of 86 soundings associated with tropical cyclone-related tornadoes.

Surface-based CAPE in the TCY sounding is 1150 J kg^{-1}. CAPE in the 0-3 km layer is 183 J kg^{-1}. These are the highest values of instability among the four categories. The CAPE values in the TCY sounding are slightly larger than that of McCaul's composite. However, it is interesting to note that this study, as well as other studies of tropical-cyclone tornadoes (Gentry 1983; McCaul and Weisman 1996) emphasized the fact that

---

[2] T03 used mean parcel CAPE (mlCAPE) in the lowest 100 mb.

the environment was less buoyant than that of a "typical" supercell environment. The current study suggests that on average, tropical cyclone environments are more buoyant than the "typical" ST environment over the GSP CWA, particularly in the low levels.

Considering that ten of the thirteen outbreak cases were identified as GRL and EPL events, it is not surprising that the outbreak sounding (Fig. 16) closely resembles the GRL and EPL composites. The outbreak sounding contains 23.8 m s^{-1} of deep layer shear. Values of 0-1 km and 0-3 km SRH are 123 m^2 s^{-2} and 240 m^2 s^{-2}, respectively. The sounding yields 849 J kg^{-1} and 93 J kg^{-1} of sbCAPE and 0-3 km CAPE, respectively. The EHI in the sounding is 1.2, equivalent to the highest EHI produced by the four composite soundings from each of the ST categories.

6. Sounding parameter climatology

Section 5 detailed the composite soundings developed for each ST category, and provided some discussion of the sounding parameters yielded by those composite or "average" soundings. This section will provide statistical analysis of various parameters derived from each of the 60 ST soundings.

A box-and-whiskers plot presenting the distribution of 0-6 km bulk wind shear for the 60 ST soundings (Fig. 17) indicates the median value of deep-layer shear is 23.3 m s^{-1}. The 1st quartile value of 0-6 km shear is 18.8 m s^{-1} while the 3rd quartile is 28.3 m s^{-1}. The maximum shear value associated with ST occurrence is 37.2 m s^{-1}. The minimum value is 5.9 m s^{-1}.

A box-and whiskers plot analyzing the values of 700 hPa to 500 hPa lapse rate is shown in Fig. 18. The median value of mid-level lapse rate is 5.9 ^{o}C km^{-1}. The majority of the lapse rate values associated with ST occurrence are within the range of 5.5 ^{o}C km^{-1} and 6.4 ^{o}C km^{-1}. The maximum value of mid-level lapse rate in the 0-6 hour period prior to ST is 7.6 ^{o}C km^{-1} while the minimum value is 4.4 ^{o}C km^{-1}.

The analysis of surface-based CAPE associated with ST occurrence (Fig. 19a) shows the mean value of sbCAPE is 977 J kg^{-1}. Values of sbCAPE are generally contained within the range of 448 J kg^{-1} (1st quartile) to 1583 J kg^{-1} (3rd quartile). The minimum value of sbCAPE associated with a ST is 33 J kg^{-1}. The maximum value is 4312 J kg^{-1}.

An analysis of CAPE in the 0-3 km layer (Fig. 19b) indicates a median value of low-level CAPE of 108 J kg^{-1}. The 0-3 km CAPE associated with ST occurrence is typically within the range of 61 J kg^{-1} and 155 J kg^{-1}. The minimum 0-3 km CAPE yielded by an ST sounding is around 0 J kg^{-1} and the maximum is 314 J kg^{-1}.

A box-and-whiskers plot presenting the distribution of 0-3 km SRH values associated with ST in the GSP CWA (Fig. 20a) reveals a median value of 182 m^2 s^{-2}. Most of the values associated with ST occurrence are in the range of 140 m^2 s^{-2} to 286 m^2 s^{-2}. The maximum value is 584 m^2 s^{-2}. The minimum value of 0-3 km SRH is 55 m^2 s^{-2}.

The analysis of 0-1 km SRH in Fig. 20b indicates the median value associated with ST occurrence is 95 $m^2 s^{-2}$. Values of 0-1 km SRH are generally contained within the range of 70 $m^2 s^{-2}$ (1st quartile) and 130 $m^2 s^{-2}$ (3rd quartile). The maximum value associated with ST is 337 $m^2 s^{-2}$. The minimum value of 0-1 km SRH is 20 $m^2 s^{-2}$.

A box-and-whiskers plot indicating the distribution of Energy Helicity Index (EHI) associated with ST occurrence (Fig. 21) indicates the median value of EHI is 1.0. Values of EHI associated with ST generally range from 0.6 to 1.4. The maximum value of EHI is 3.6. The minimum value is 0.1.

Distribution of Bulk Richardson Number (BRN) associated with ST occurrence in the GSP CWA (Fig. 22) indicates the median value of BRN is 11.5. Values of BRN typically range from 5.0 (1st quartile) to 23.0 (3rd quartile). The maximum value of BRN associated with ST is 140.0 and the minimum is 0.0.

Examination of Table 2 reveals shear parameters are comparable to previous climatological studies of tornadic convection, especially for 0-3 km SRH and 0-6 km bulk shear. However, the mean value of CAPE associated with ST in the GSP CWA is less than half that in T03 whereas the mean value of 0-3 km CAPE in the current study (117 J kg^{-1}) is approximately 45% *greater* than in R03. This suggests that the initial acceleration of the updraft may be more important than the overall strength and depth of the updraft in dictating the tornadic potential of a thunderstorm, at least in the GSP CWA.

7. Summary

A climatology was developed for all of the ST that have occurred across the GSP CWA since 1880. ST are most common from March through May during the late afternoon and early evening. It was found that ST are most common along the I-85 corridor of northeast Georgia, Upstate South Carolina, and the North Carolina Piedmont. However, this result is believed to be partially biased by the high population density of this area. ST within the GSP CWA are much less common across far western North Carolina, where the rugged terrain is assumed to play a major role in hindering ST occurrence. Finally, it is hypothesized that the mountains also play a role in the relative infrequency of ST downstream over the foothills and northern Piedmont of North Carolina. However, the lee trough may occasionally provide a low-level focus for tornadic convection. Therefore, the mountains could play an indirect role in enhancing the tornadic potential in certain situations.

A database of all ST within the Greenville-Spartanburg, SC (GSP) County Warning Area has been compiled using various resources. For each "ST day" since 1948 (a total of 60 days), NCEP reanalysis data have been examined within the 0-6 hour window prior to ST occurrence across the GSP CWA. Four categories of "ST days" have been identified based upon the position of surface low pressure prior to the occurrence of ST. Composite analyses of NCEP-NCAR reanalysis data have been developed for each of the four categories in an attempt to illustrate the "average" synoptic conditions associated with ST occurrence. The composites reveal that ST typically occur when the GSP CWA is located

well within the warm sector of an extratropical cyclone (i.e., surface low pressure is located from 300 km to 1500 km northwest of the CWA.) It is hypothesized that this pattern has important implications for preventing establishment of a surface-based stable air mass associated with cold air damming. Another pattern sometimes associated with ST occurrence is the presence of a landfalling tropical cyclone near the central Gulf Coast. Despite the differences in the location of key synoptic features, one characteristic shared by most of the composite analyses is the superimposition of a maximum in 850 hPa wind speed with a maximum in 850 hPa moisture. This would seem to suggest that environmental characteristics of the lowest 2 or 3 km are most important in influencing development of ST.

For each of the 60 ST days, a sounding was constructed from NCEP-NCAR reanalysis data at the gridpoint deemed to be most representative of the tornadic environment. Various instability and wind shear parameters were documented for each sounding. From these individual soundings, a composite sounding was developed for each ST category. In most of the categories, values of SRH and bulk wind shear were comparable to previous studies of proximity soundings associated with ST. Instability parameters were often significantly lower than in other studies, particularly with regard to deep layer instability. However, values of composite CAPE in the 0-3 km layer were comparable, and in some cases larger, than those in previous studies. This seems to strengthen the notion that the character of the environment in the lowest 3 km may be very important in distinguishing ST environments from non-ST environments.

References

Bailey, C. M., G. Hartfield, G. M. Lackmann, K. Keeter, and S. Sharp, 2003: An objective climatology, classification scheme, and assessment of sensible weather impacts for Appalacian cold-air damming. *Wea. Forecasting*, **18**, 641-661.

Barnes, S. L., and C. W. Newton, 1983: Thunderstorms in the synoptic setting. *Thunderstorm Morphology and Dynamics*, E. Kessler, Ed., University of Oklahoma, 75–112.

Bell G. D., and L. F. Bosart, 1988: Appalachian cold-air damming. *Mon. Wea. Rev.*, **116**, 137–161.

Doswell, C.A., III, and D.W. Burgess, 1988: On some issues of United States tornado climatology. *Mon. Wea. Rev.*, **116**, 495-501.

_____, S.J. Weiss, and R.H. Johns, 1993: Tornado forecasting: A review. *The Tornado: Its Structure, Dynamics, Prediction, and Hazards* (C. Church et al., Eds), Geophys. Monogr. 79, Amer. Geophys. Union, 557-571.

Gentry, R.C., 1983: Genesis of tornadoes associated with hurricanes. *Mon. Wea. Rev.*, **111**, 1793-1805.

Grazulis,T.P., 1993: *Significant Tornadoes*, 1680-1991. Environmental Films, St.Johnsbury, VT, 1326 pp.

Hart, J. A., 2005; Local severe weather climatologies for WSR-88D radar areas across the United States. *Presentations of the 30th National Weather Association Annual Meeting.* St. Louis, MO. [see: http://www.spc.noaa.gov/climo/online/rda/]

Kelly, D.L., J.T. Schaefer, R.P. McNulty, C.A. Doswell III, and R.F. Abbey, Jr., 1978: An augmented tornado climatology. *Mon. Wea. Rev*., **106**, 1172-1183.

Kistler, R., E. Kalnay, W. Collins, S. Saha, G. White, J. Woollen, M. Chelliah, W. Ebisuzaki, M. Kanamitsu, V. Kousky, H. van den Dool, R. Jenne, and M. Fiorino, 2001: The NCEP-NCAR 50-Year Reanalysis: Monthly Means CD-ROM and Documentation. *Bull. Amer. Meteor. Soc*., **82**, 247-268.

Lackmann, G. M., and W. M. Stanton, 2004: Cold-air damming erosion: Physical mechanisms, synoptic settings, and model representation. Preprints, *20th Conf. on Weather Analysis and Forecasting*, Seattle, WA, Amer. Meteor. Soc., CD-ROM, 18.6.

McCaul, E.W., Jr., 1991: Buoyancy and shear characteristics of hurricane-tornado environments. *Mon. Wea. Rev*., **119**, 1954-1978.

McCaul, E.W., Jr., and M.L. Weisman, 1996: Simulations of shallow supercell storms in landfalling hurricane environments. *Mon. Wea. Rev*., **124**, 408-429.

Miller, R.C., 1972: Notes on the analysis and severe-storm forecasting procedures of the Air Force Global Weather Central, *Tech. Rep. 200,* 190 pp., Air Weather Serv., Scott Air Force Base, Ill.

Novlan, D.J., and W.M. Gray, 1974: Hurricane spawned tornadoes. *Mon. Wea. Rev*., **102**, 476-488.

Parker, M. D., and D. A. Ahijevych, 2007: Convective episodes in the east-central United States. *Mon. Wea. Rev*., **135**, 3707-3727.

Rasmussen, E.N., 2003: Refined supercell and tornado forecasting parameters. *Wea. Forecasting*, **18**, 530-535.

_____ , and D.O. Blanchard, 1998: A baseline climatology of sounding-derived supercell and tornado forecast parameters. *Wea. Forecasting*, **13**, 1148-1164.

Schaefer, J.T., R.L. Livingston, F.P. Ostby, and P.W. Leftwich (1993): The stability of climatological tornado data. *The Tornado: Its Structure, Dynamics, Hazards, and Prediction* (Geophys. Monogr. 79), Amer. Geophys. Union, 459-466.

Thompson, R.L., R. Edwards, J.A. Hart, K.L. Elmore, and P. Markowski, 2003: Close
proximity soundings within supercell environments obtained from the rapid
update cycle. *Wea. Forecasting*., **18**, 1243-1261.

Weisman, R.A., 1990: An Observational Study of Warm Season Southern Appalachian
Lee Troughs. Part II: Thunderstorm Genesis Zones. *Mon. Wea. Rev*., **118**, 2020–2041.

Acknowledgments
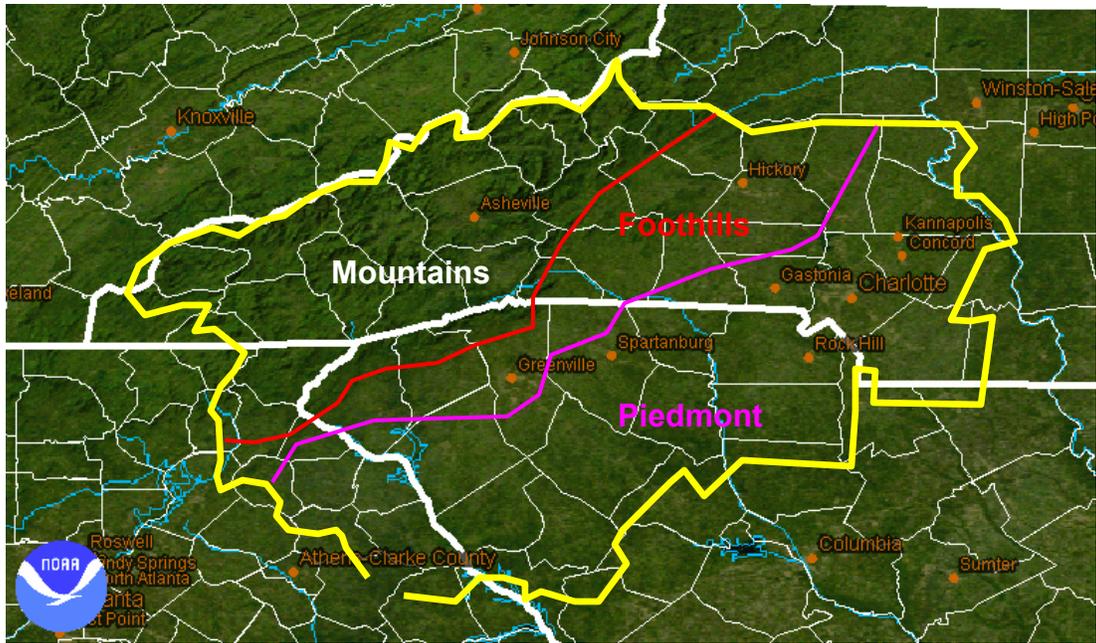
Figure 1. Topographic map of the Greenville-Spartanburg, SC County Warning Area (CWA). Heavy white lines are state boundaries. Light white lines are county borders. Yellow line is the outline of the CWA. CWA land left of the red line is mountainous. Area to the right of the purple line is the piedmont. The foothills are in between the red and purple lines.
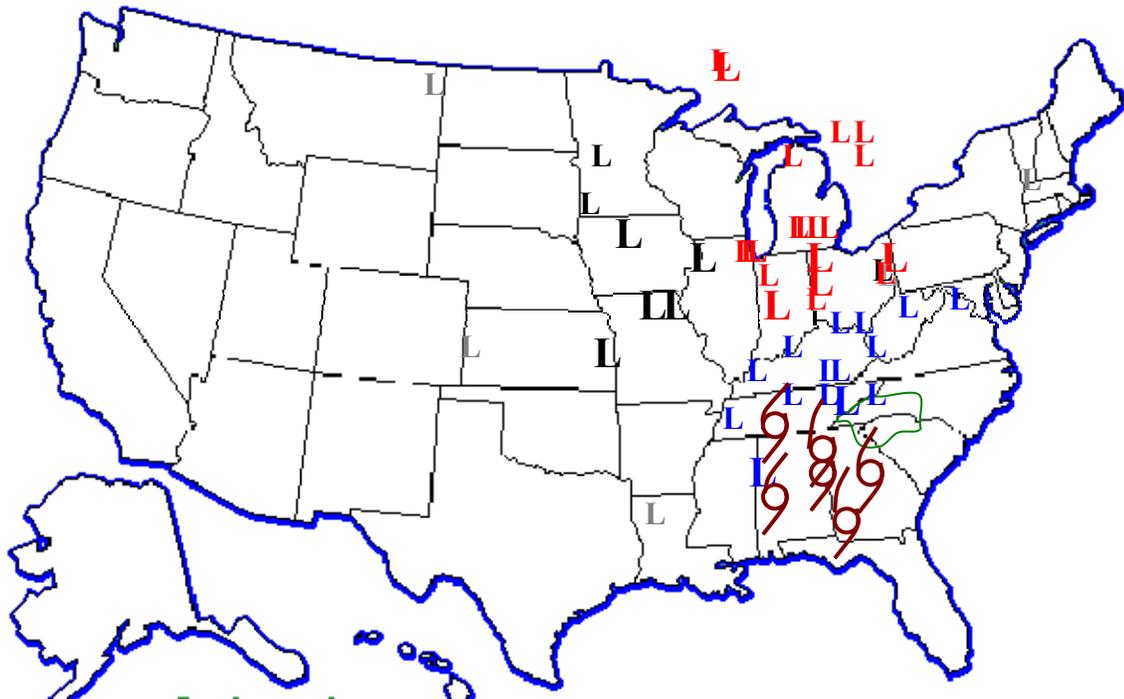

Figure 2. Map illustrating the position of the synoptic low pressure center in the 0-6 hour window prior to significant tornado occurrence in the GSP CWA. Brown circles with curved lines represent tropical cyclones. "Ls" represent locations of surface low pressure. Map labels are color-coded according to ST synoptic category. Red represents Great Lakes (GRL). Blue is Ohio/Tennessee Valley (OTV). Black is Eastern Great Plains (EPL). Lows with a gray font were not included in any of the four categories.
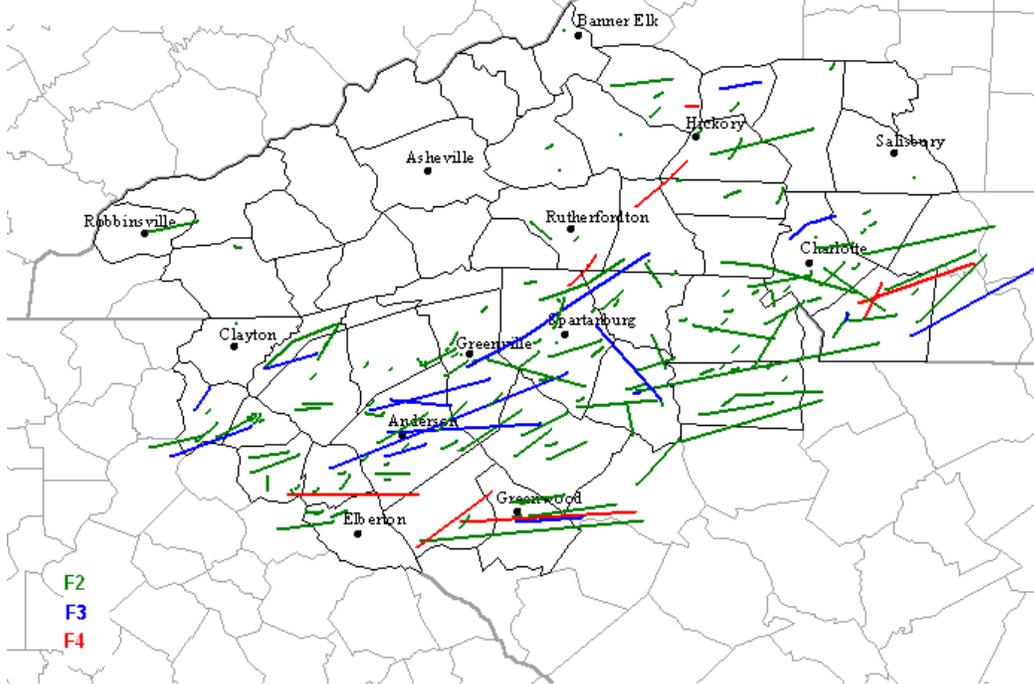
Figure 3. Tracks of significant tornadoes in the GSP CWA (1880-2006). F2 tracks are in green. F3 tracks are in blue. F4 tracks are in red.
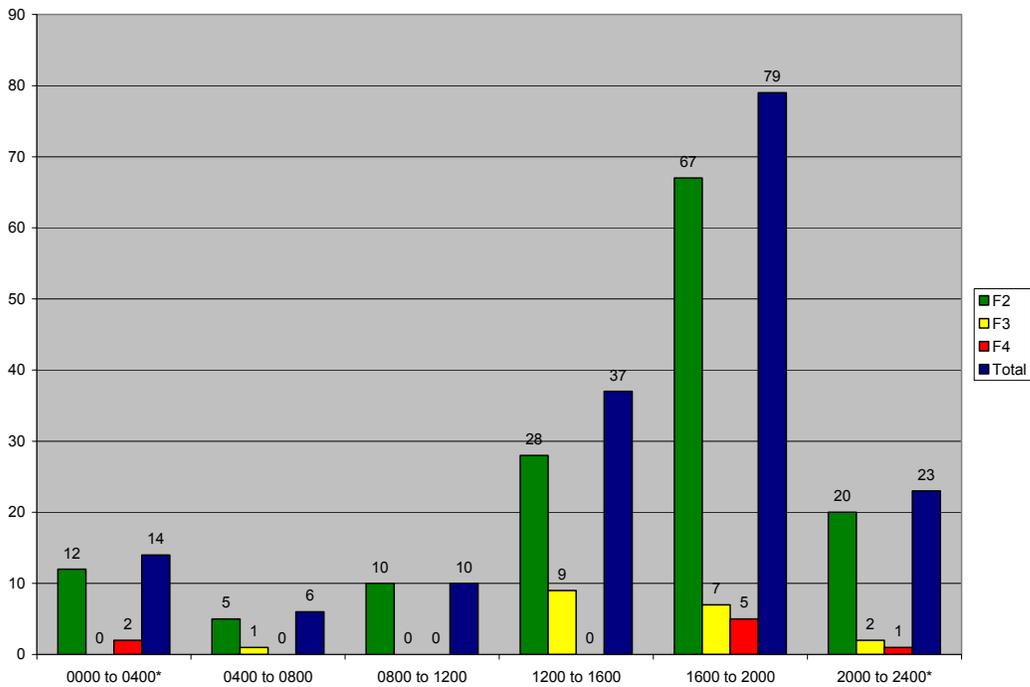

Figure 4. Diurnal distribution of significant tornadoes in the GSP CWA (1880-2006).
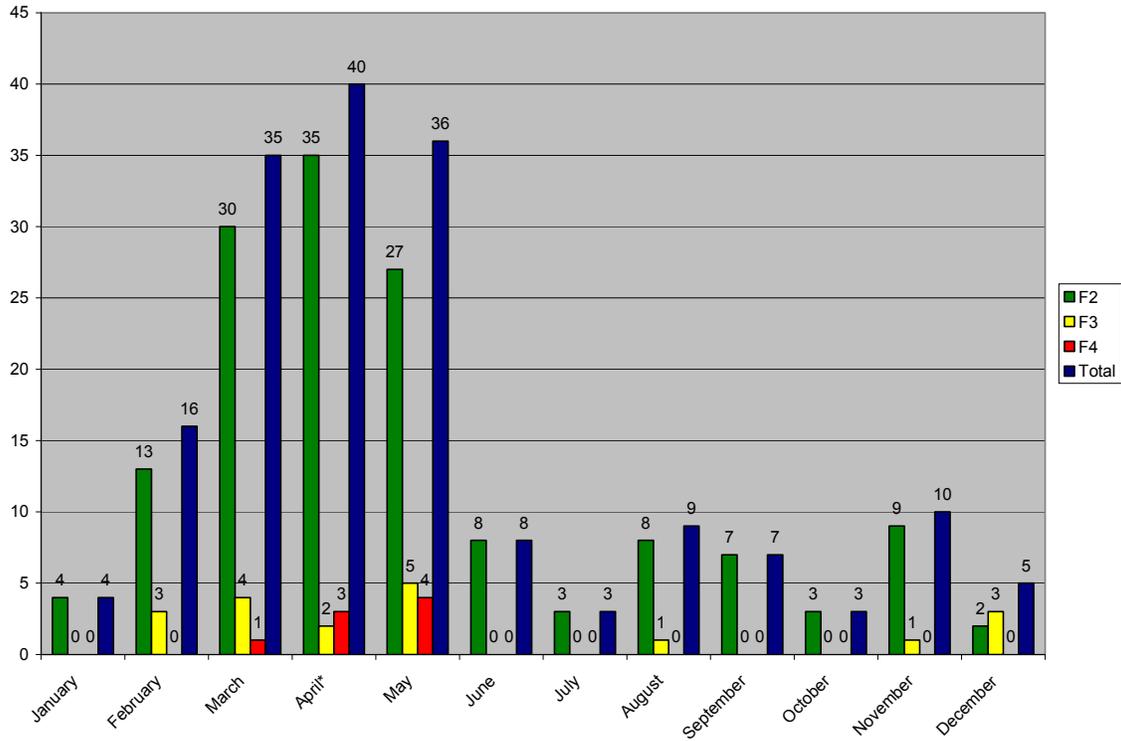
Figure 5. Monthly distribution of significant tornadoes in the GSP CWA (1880-2006).
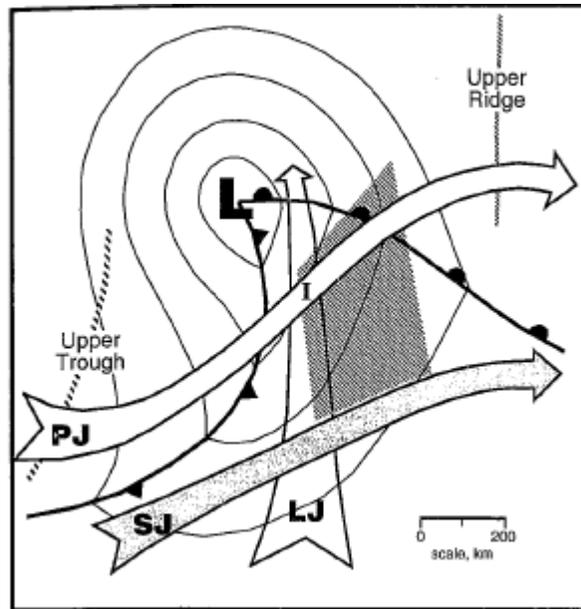
Figure 6. Idealized composite map of major synoptic scale features typically associated with severe weather outbreaks. "L" is the location of surface low pressure. "PJ" is the Polar branch of the upper level jet. "SJ" is the subtropical branch of the upper jet. "LJ" represents the location of the low level jet. Adapted from Barnes and Newton (1983).
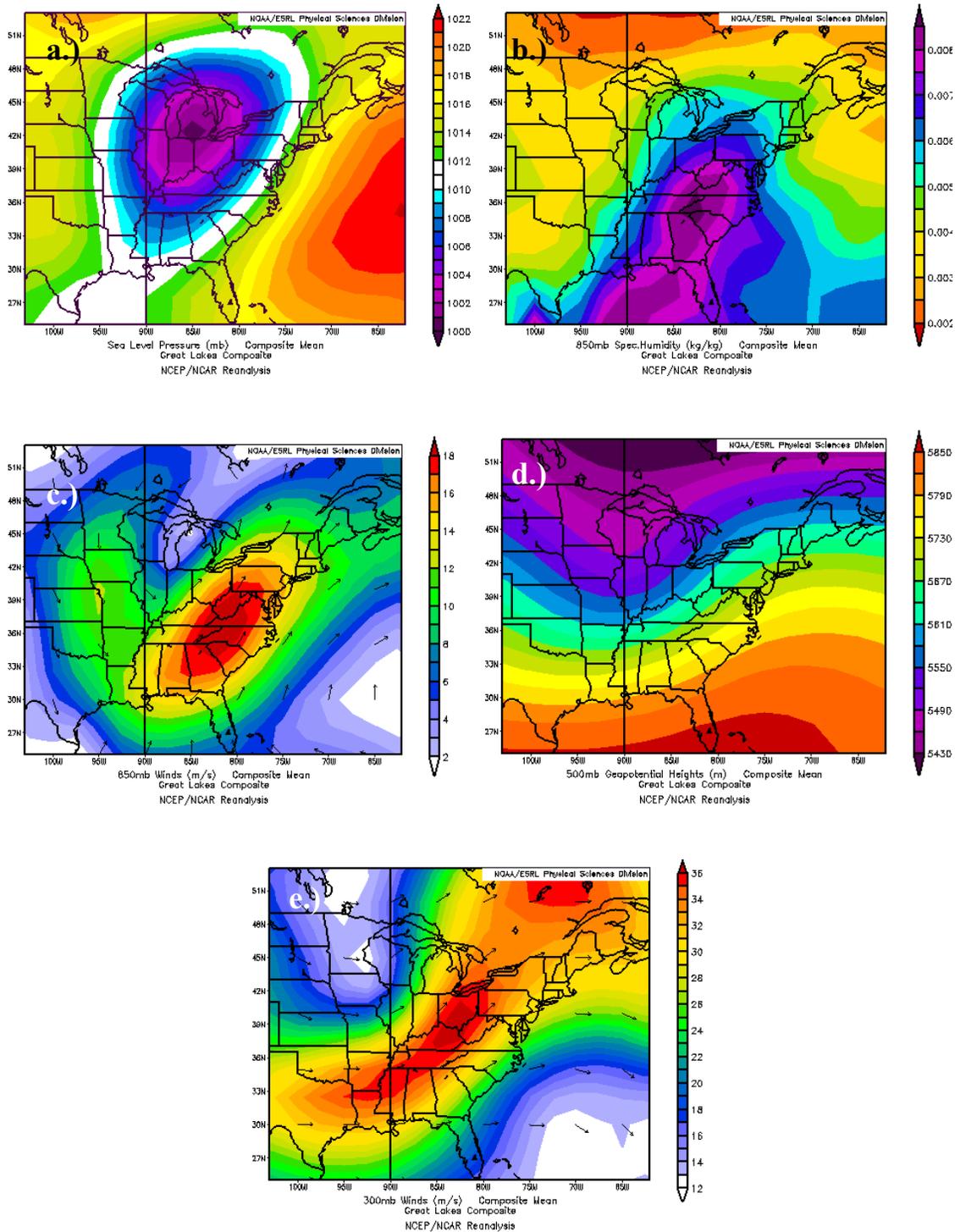
Figure 7. Composite analysis of a) sea level pressure b) 850 hPa specific humidity c) 850 hPa wind speed d) 500 hPa geopotential height and e) 300 hPa wind speed for the Great Lakes ST synoptic category.

19
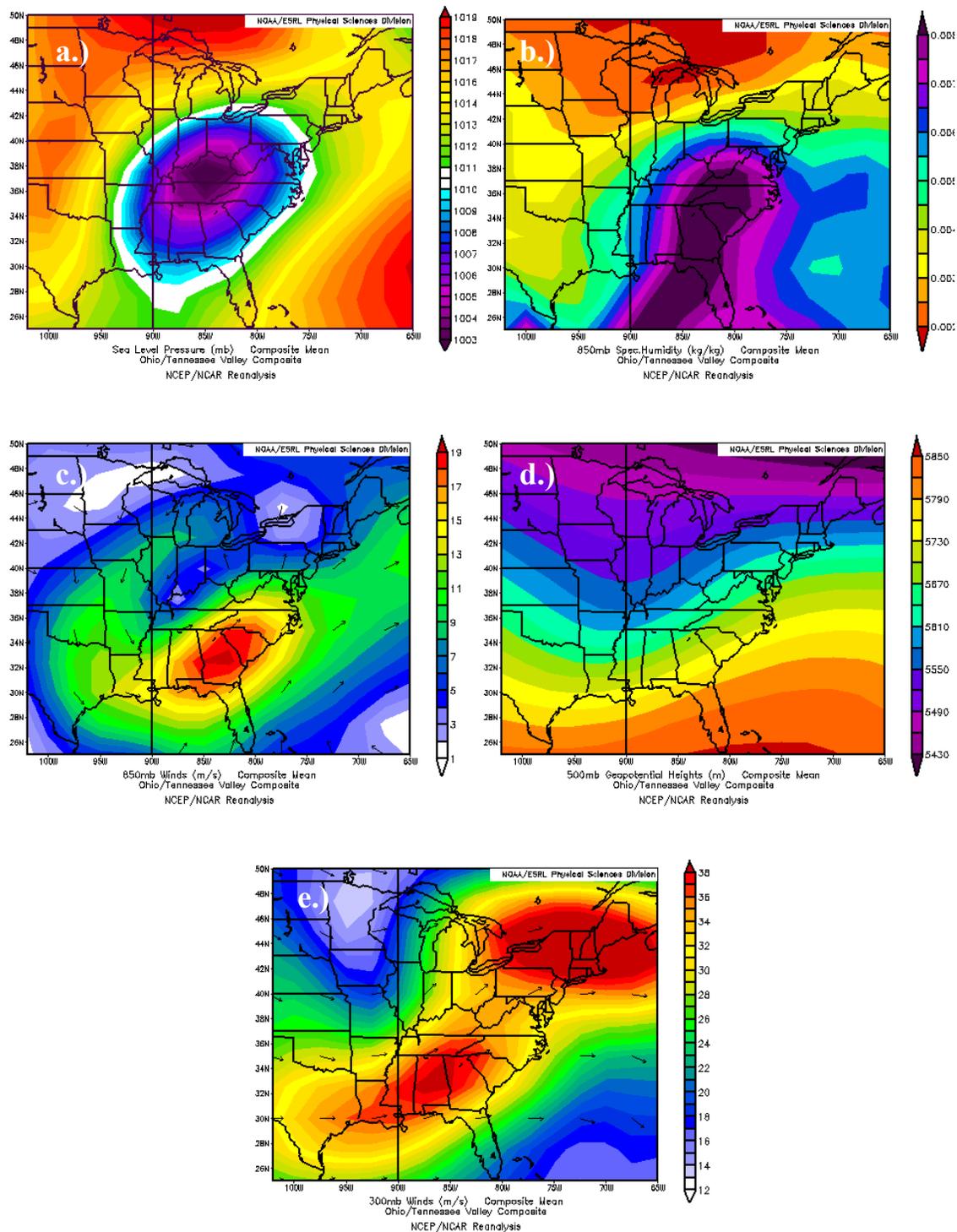
Figure 8. Same as in Fig. 7 except for the Ohio/Tennessee Valley ST synoptic category.
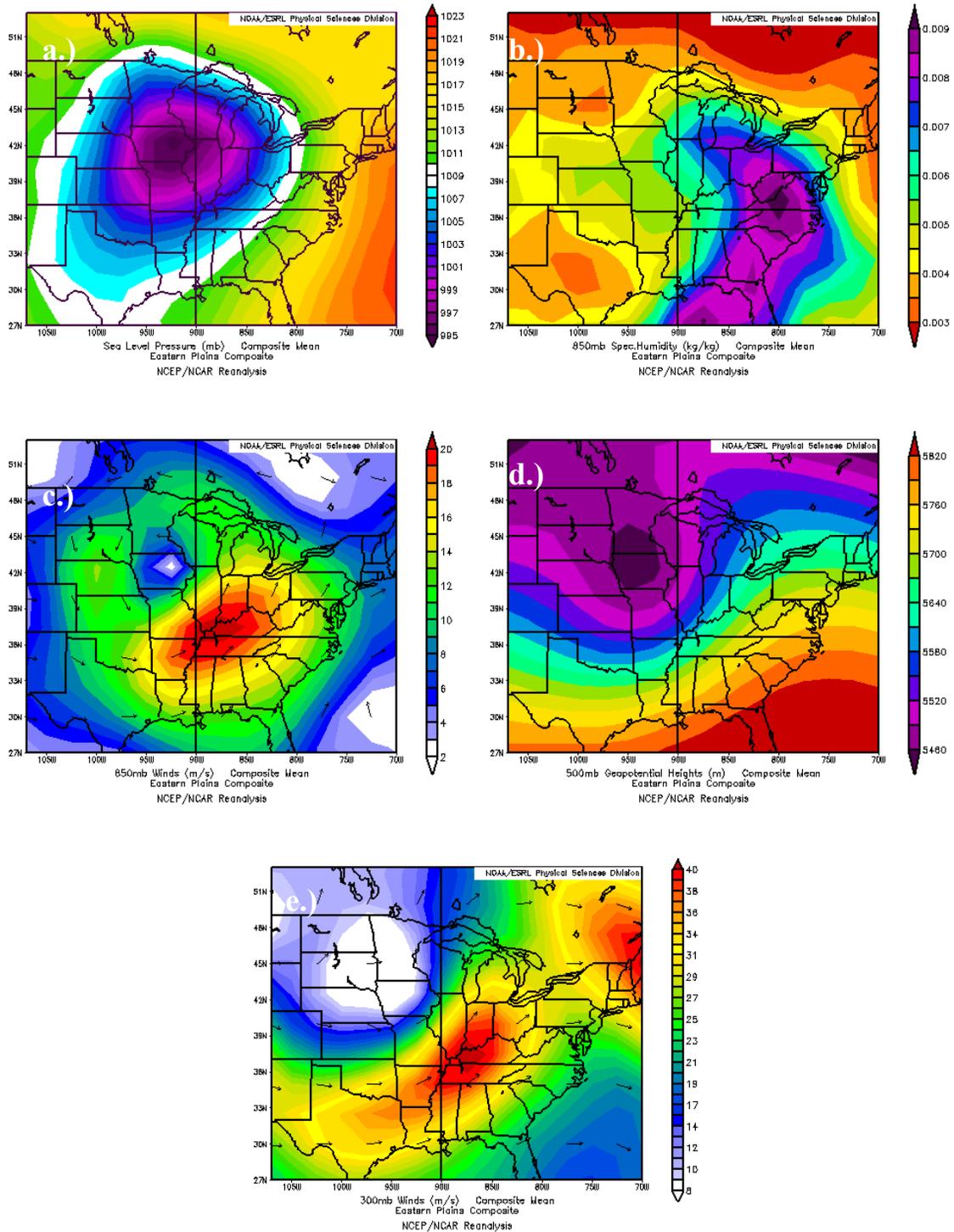
Figure 9. Same as in Fig. 7 except for the Eastern Plains (EPL) ST synoptic category.
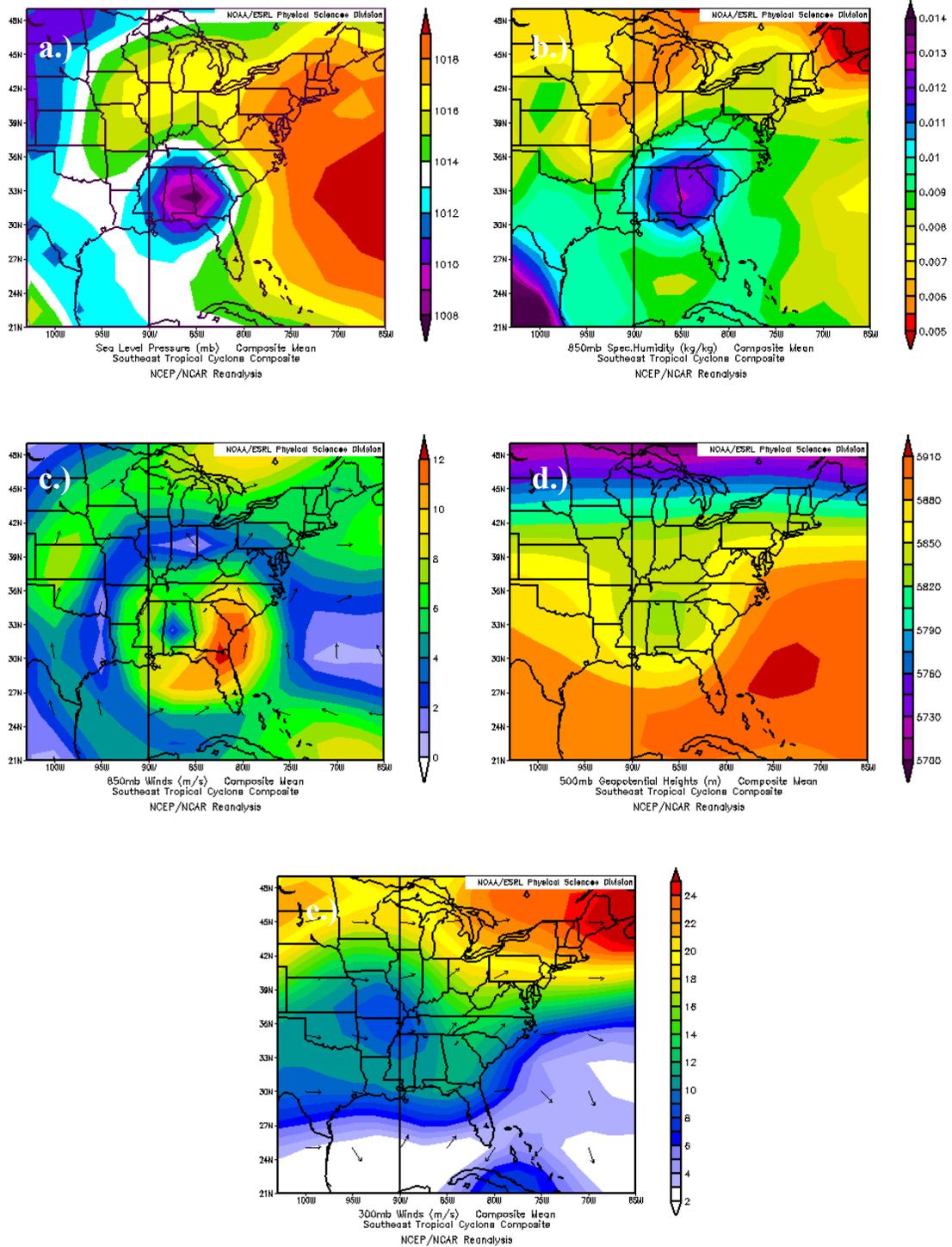
Figure 10. Same as in Fig. 7 except for Southeast Tropical Cyclone ST synoptic category.
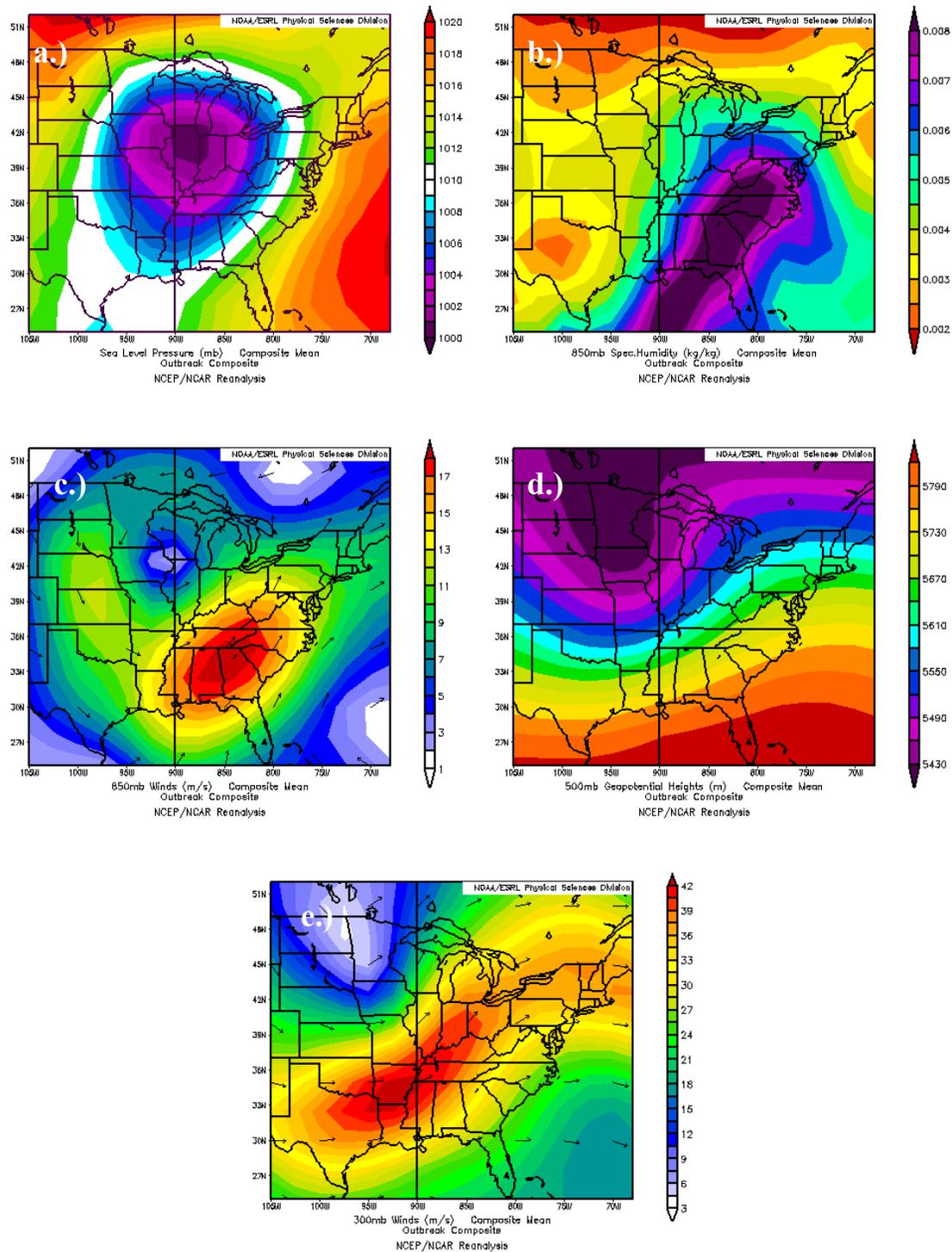
Figure 11. Same as in Fig. 7 except for ST outbreak days.
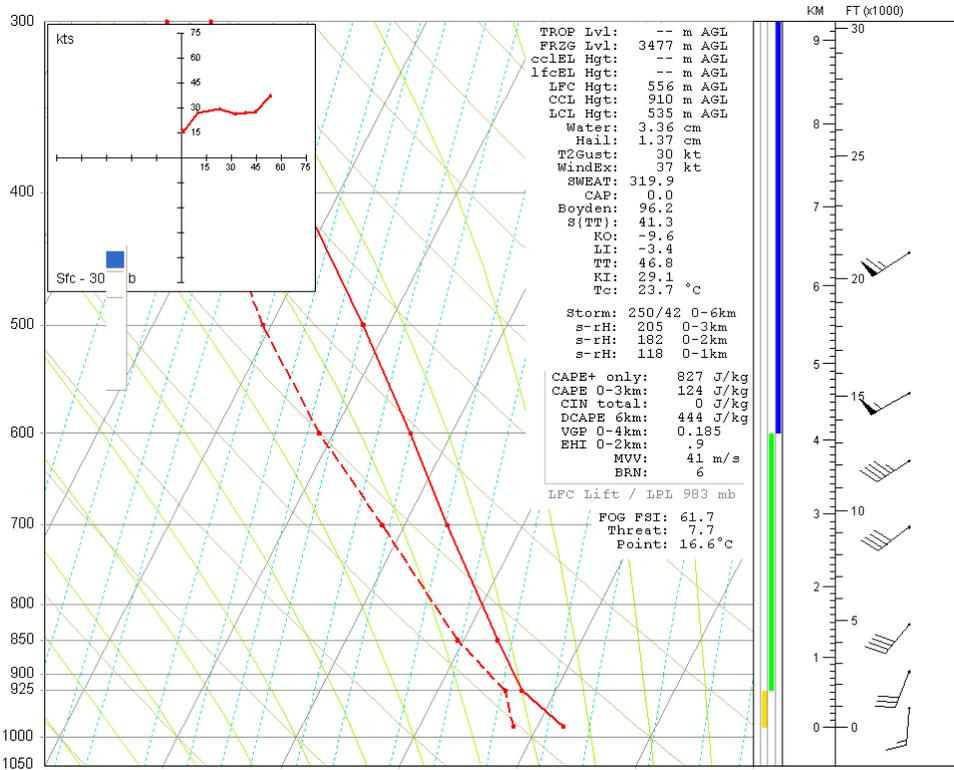
Figure 12. Skew-T/log p diagram representing the composite sounding for the Great Lakes (GRL) ST synoptic category.
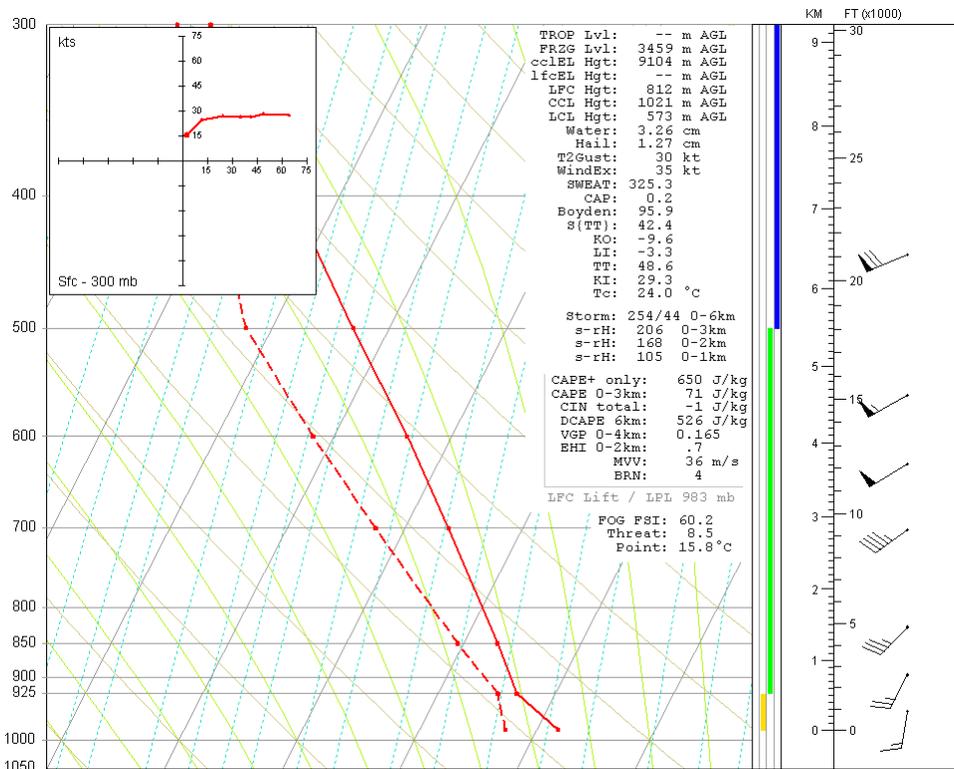
Figure 13. Same as in Fig. 12 except for the Ohio/Tennessee Valley (OTV) composite.
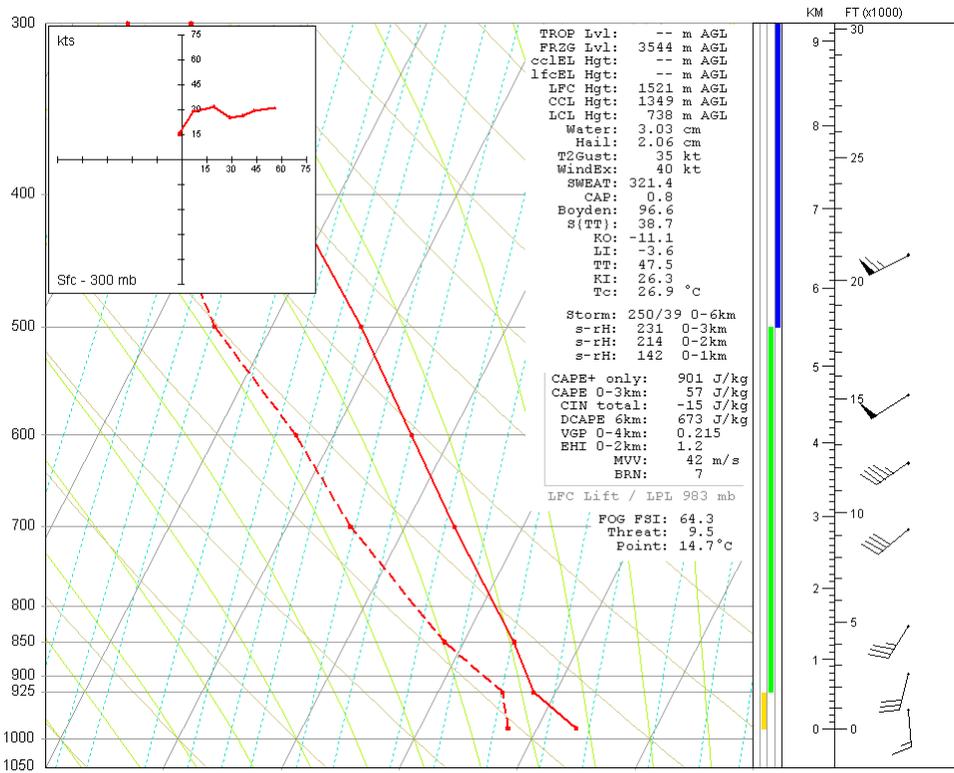
Figure 14. Same as in Fig. 12 except for the Eastern Great Plains (EPL) category.
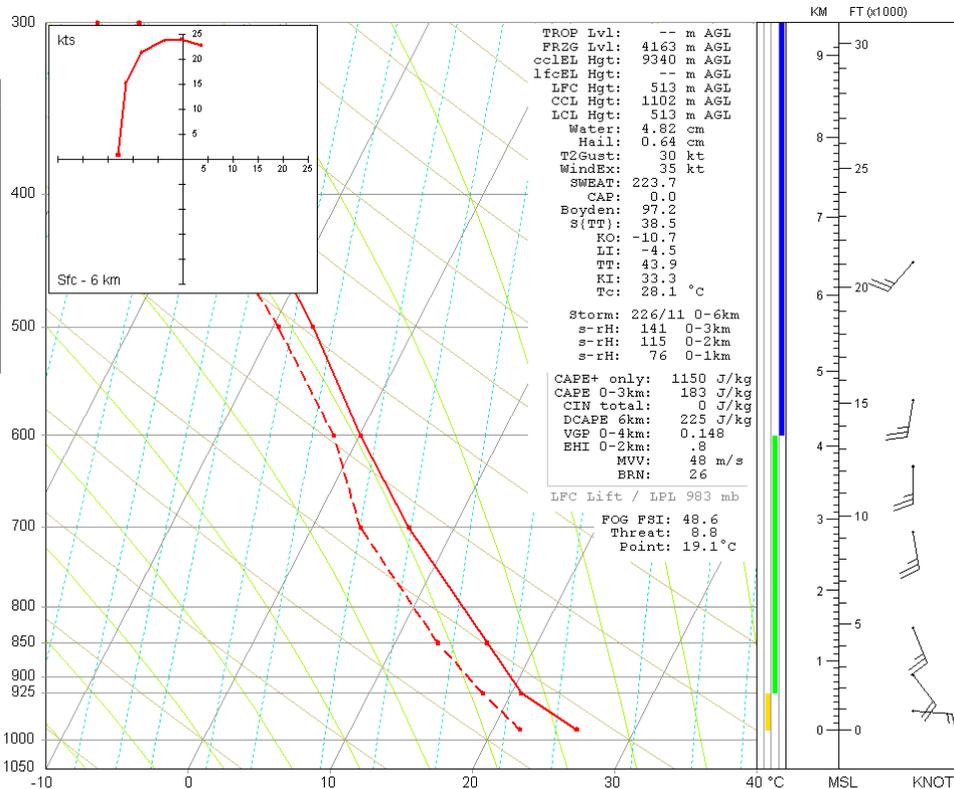
Figure 15. Same as in Fig. 12 except for the Southeast Tropical Cyclone (TCY) category.

25
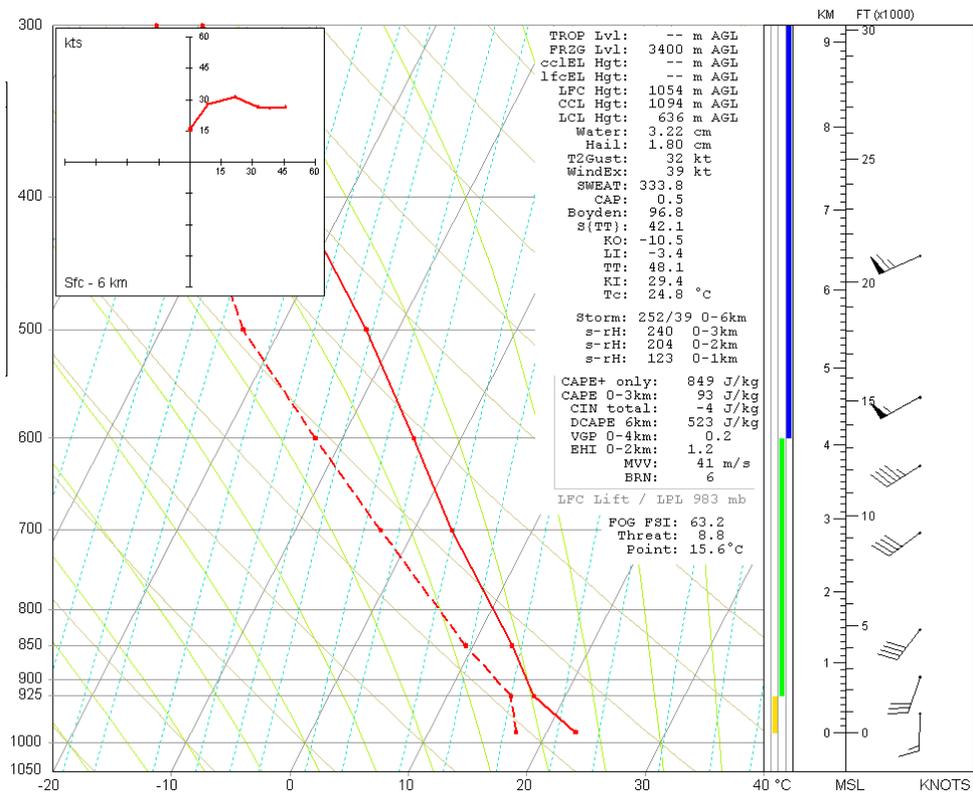
Figure 16. Same as in Fig. 12 except for ST outbreak days.
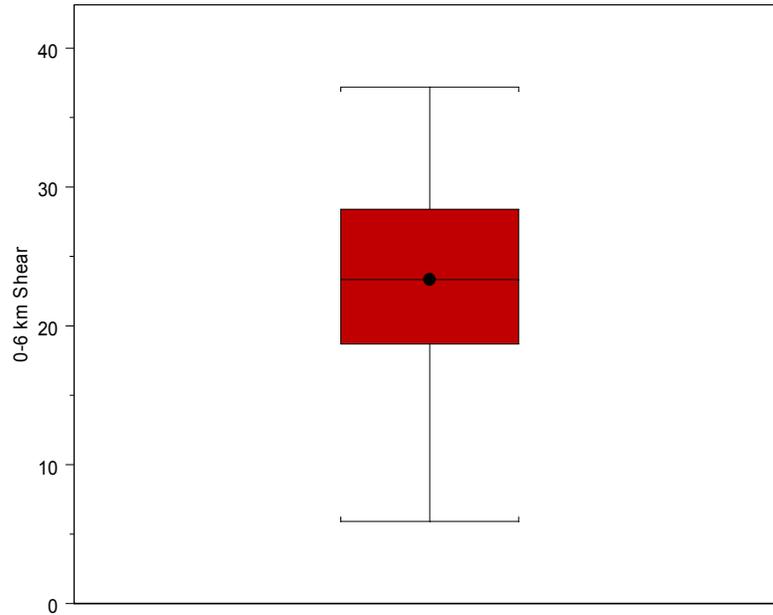
Figure 17. Box and whiskers graph of 0-6 km wind shear (m s^{-1}) from the 60 ST soundings. Red box denotes the 25th to 75th quartile, with horizontal bar and red dot marking the median value. Vertical lines extend from the box to the 10th and 90th percentile. Dot outside of the box plot represents an outlier.
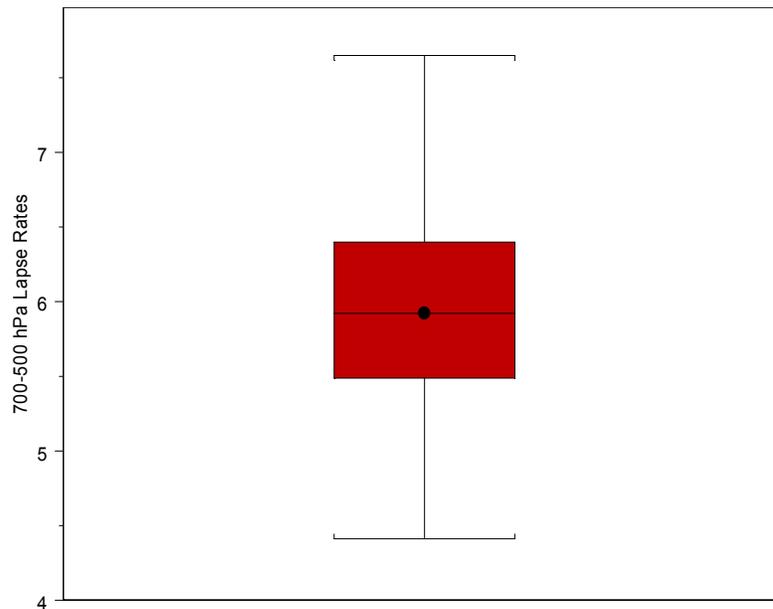
Figure 18. Same as in Fig. 17 except for 700 hPa to 500 hPa lapse rates (^{o}C km^{-1}).

a)

b)
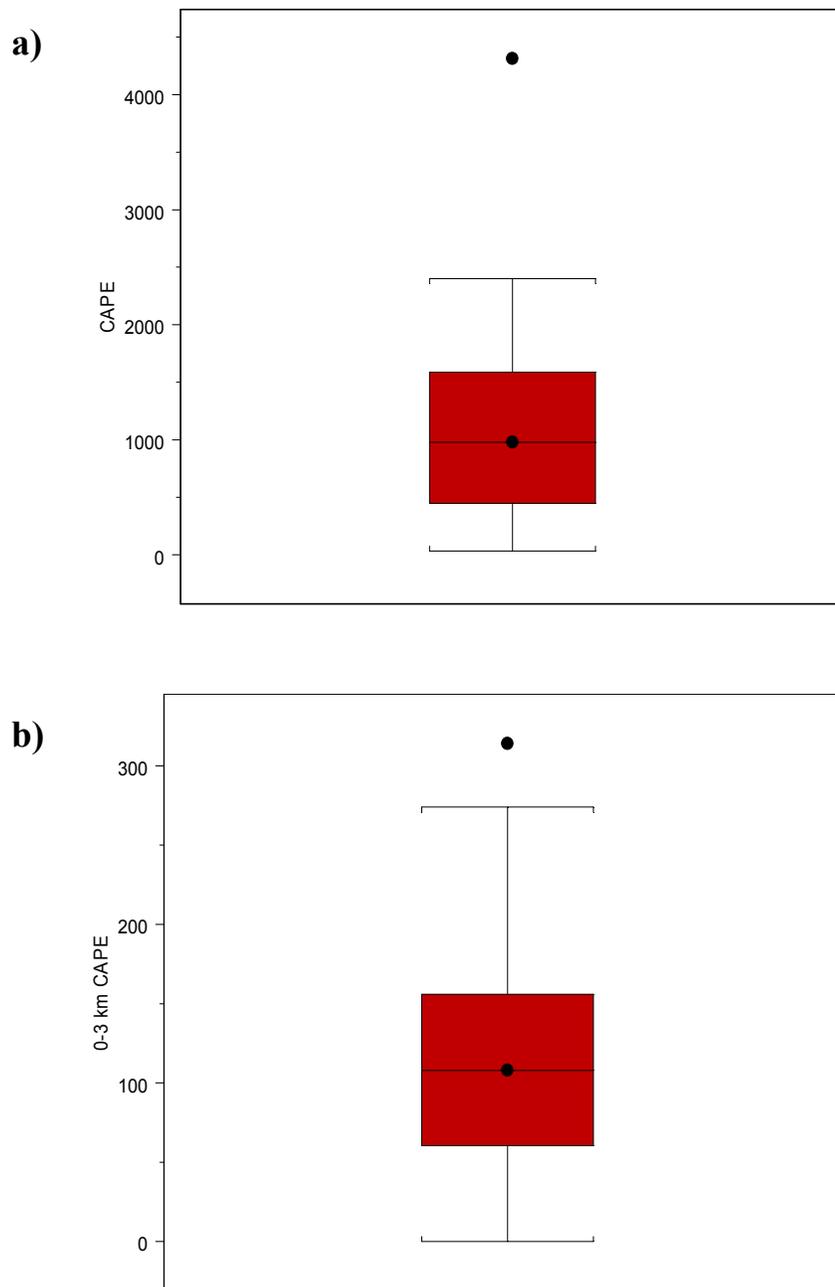
Figure 19. Same as in Fig. 17 except for a) Surface-based CAPE and b) 0-3 km CAPE (J kg^{-1}).
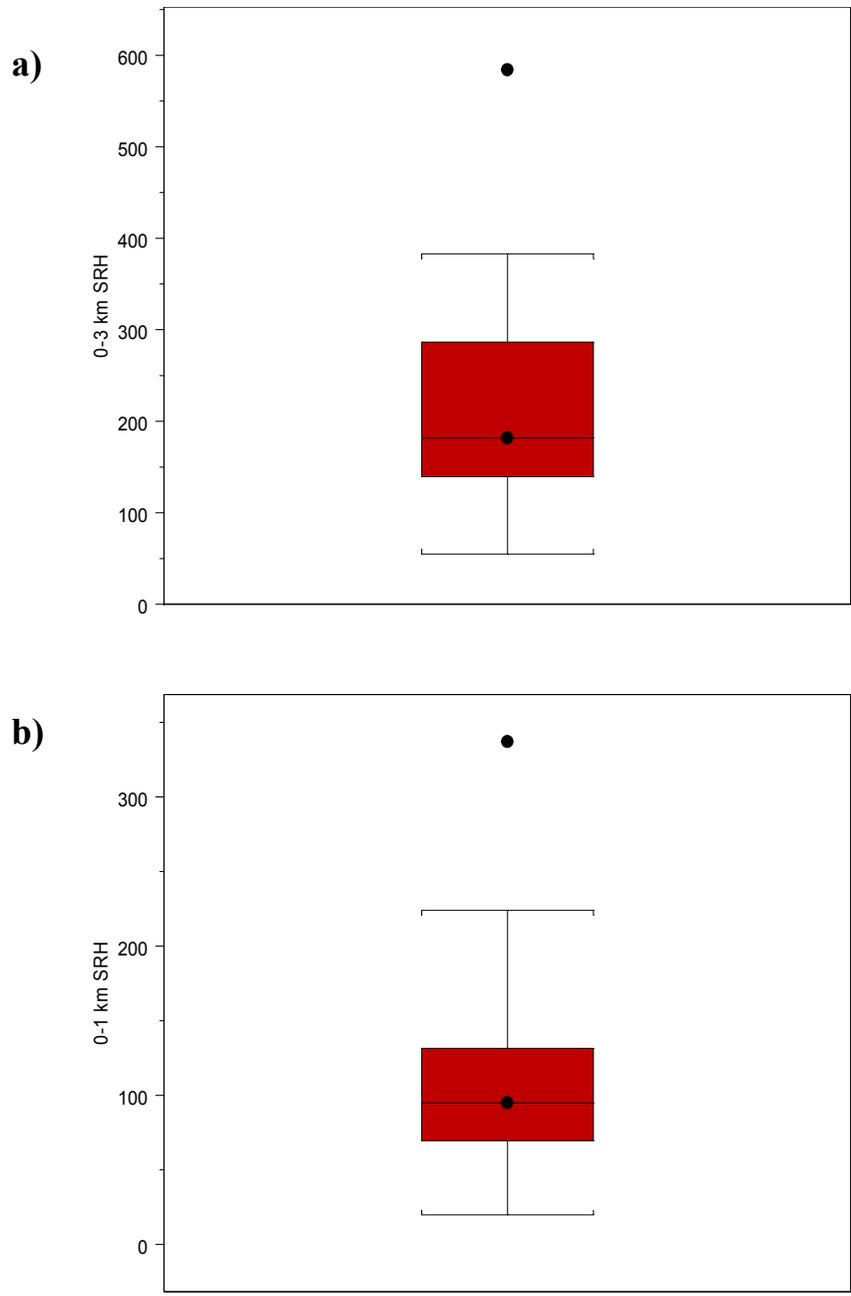
Figure 20. Same as in Fig. 17 except for a) 0-3 km Storm Relative Helicity and b) 0-1 km Storm Relative Helicity (m^2 s^{-2}) .
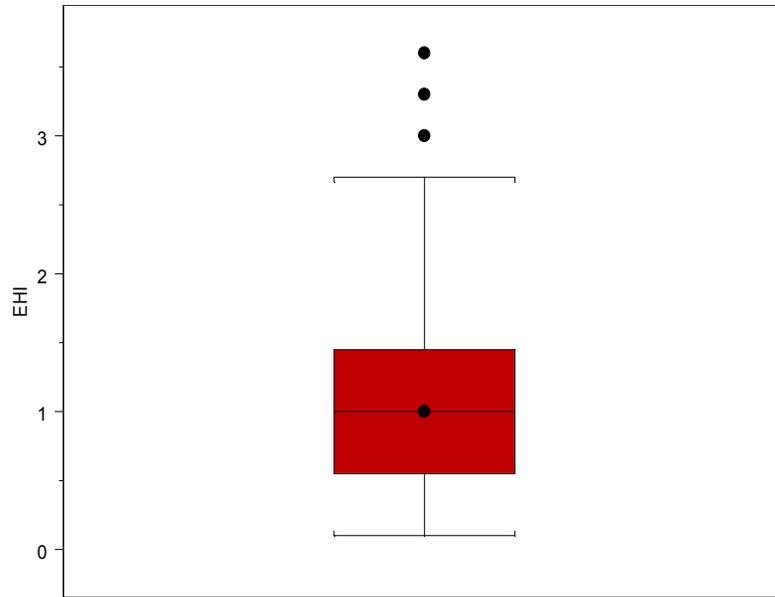
Figure 21. Same as in Fig. 17 except for Energy Helicity Index.
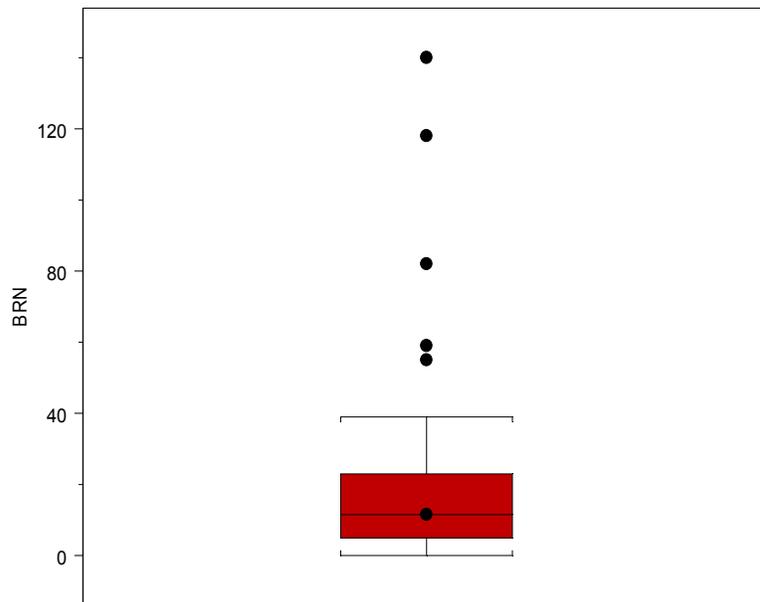
Figure 22. Same as in Fig. 17 except for Bulk Richardson Number.

Table 1. Significant tornadoes in the Greer, SC County Warning and Forecast area from 1880-2006.

| DATE	TIME (EST)	COUNTY	F-SCALE	FATAL	INJ
3-Apr-1880	Unk	Elbert	2	0	0
3-Apr-1880	2345	Habersham/Stephens	2	3	20
19-Feb-1884	1530	Hall/Banks/Habersham/Stephens	3	2	20
19-Feb-1884	1630	Spartanburg	2	0	6
19-Feb-1884	1730	Anderson	3	2	20
19-Feb-1884	1815	Fairfield/Chester/Lancaster	2	3	10
19-Feb-1884	1830	Greenwood/Newberry	2	5	30
19-Feb-1884	2000	Union, NC/Anson/Richmond/Montgomery	3	4	50
19-Feb-1884	2100	Cabarrus/Stanly/Montgomery	2	1	25
25-Mar-1884	Unk	Lincoln	2	0	Unk
25-Mar-1884	Unk	Caldwell	2	1	5
25-Mar-1884	Unk	Mecklenburg	2	0	5
25-Mar-1884	1600	Greenville	2	1	2
25-Mar-1884	1600	Oconee/Anderson/Greenville	3	9	40
25-Mar-1884	1700	Catawba/Iredell	2	2	14
25-Mar-1884	1700	York	2	0	5
25-Mar-1884	1800	York	2	0	15
25-Mar-1884	1800	Chester	2	1	8
25-Mar-1884	1845	Macon	2	Unk	Unk
27-May-1885	1530	Spartanburg	2	Unk	Unk
27-May-1885	1545	York	2	0	0
15-Apr-1886	1800	Rutherford	2	0	5
26-Nov-1886	Unk	York	2	0	Unk
4-Aug-1888	1500	McDowell	2	Unk	Unk
15-Sep-1888	1730	Anderson	2	0	0
18-Feb-1889	530	Spartanburg	2	0	4
1-May-1889	1700	Cherokee/Cleveland	2	0	Unk
22-Mar-1890	1500	Newberry/Union, SC	2	0	1
22-Mar-1890	1500	Union, SC/Chester/York/Lancaster/Union, NC	2	0	3
13-Sep-1892	1500	Newberry/Union, SC	2	0	2
29-May-1893	300	Anderson	2	3	10
21-May-1901	530	Chester/York	2	0	15
25-May-1902	1600	Union, SC	3	3	7
16-Feb-1903	1530	Anderson/Greenville/Laurens	2	3	10
16-Feb-1903	1530	Laurens	2	1	5
13-Apr-1903	1000	Elbert	2	0	0
25-Mar-1909	45	Greenwood	2	1	Unk
30-Apr-1909	Unk	Hart	2	Unk	Unk
27-May-1913	1530	Anderson	2	0	5
15-Oct-1914	1445	Cabarrus	2	0	15
20-Aug-1915	1730	Greenville	2	1	15
15-Jul-1916	Unk	Union, SC	2	0	0
22-May-1917	1830	Abbeville/Greenwood/Saluda/Newberry	2	0	9
29-Oct-1917	2130	Chester	2	0	10

11-Jan-1918	1700	Chester	2	1	3
5-Mar-1919	1730	Chester	2	0	3
2-Apr-1920	600	Chester/Lancaster	2	0	0
12-Apr-1920	1600	Oconee	2	0	10
12-Apr-1920	2100	Union, NC/Anson/Stanly	4	3	20
21-Apr-1920	300	Anderson	2	0	0
22-Apr-1920	30	Spartanburg	2	0	0
14-Jun-1920	1630	Greenville	2	0	2
20-Jun-1920	1400	Union, NC	2	0	5
18-May-1922	1845	Alexander	3	0	6
13-Apr-1923	1600	Greenville	2	0	0
30-Apr-1924	715	Hart/Anderson/Greenville/Laurens/Spartanburg	3	9	150
30-Apr-1924	900	Hall/Habersham	2	0	4
30-Apr-1924	900	Union, SC/Cherokee/York	2	0	3
26-Nov-1926	1630	York	2	1	12
29-Jun-1928	1900	Spartanburg	2	0	7
29-Jun-1928	2130	Pickens	2	0	2
13-Mar-1929	2030	Pickens	3	9	10
22-Mar-1929	1700	York/Mecklenburg	2	1	8
22-Mar-1929	1800	Cabarrus	2	0	10
25-Apr-1929	1545	Anderson/Greenville	3	6	60
4-Feb-1930	1930	Mecklenburg	2	0	0
24-Jun-1930	1900	Anderson	2	0	1
22-Mar-1932	100	Spartanburg	2	2	30
22-Mar-1932	130	Cherokee	2	1	5
7-Jun-1932	1730	Chester	2	0	0
5-May-1933	1430	Anderson/Greenville/Laurens	3	19	100
25-Mar-1935	1500	Mecklenburg/Cabarrus	2	0	1
12-Nov-1935	1645	Anderson	2	0	5
6-Apr-1936	1000	Franklin	2	1	6
6-Apr-1936	955	Anderson	2	1	30
21-Feb-1937	1737	Mecklenburg	2	0	1
20-Mar-1937	1820	Cherokee	2	0	7
20-Mar-1937	1920	York	2	0	0
15-Feb-1939	630	Pickens	2	0	1
17-Aug-1939	1400	Greenville	2	0	0
1-Dec-1942	1730	Hart	2	0	0
11-Apr-1944	1625	Stephens	2	0	5
11-Apr-1944	1800	Oconee	2	1	0
16-Apr-1944	30	Franklin/Hart/Elbert/Anderson/Abbeville	4	25	120
16-Apr-1944	100	Abbeville/Greenwood/Newberry	4	16	200
17-Apr-1945	1200	Mecklenburg	2	0	8
10-May-1945	1545	Anderson	2	1	2
23-Mar-1948	1816	Mecklenburg/Cabarrus	3	0	1
14-May-1950	1830	Union, NC	2	0	5
10-May-1952	1500	Franklin	2	0	0
31-Mar-1954	1615	Greenville/Spartanburg	3	2	4
18-Aug-1954	1600	Madison, GA/Elbert	2	0	5
28-Nov-1954	2130	Catawba	2	0	0
6-Apr-1956	1330	Cabarrus	2	0	0

6-Apr-1956	1430	Abbeville	2	0	4
8-Apr-1957	1600	Gaston/Mecklenburg/Union, NC	2	0	0
30-Mar-1960	1800	Spartanburg/Union, SC	2	0	2
9-Apr-1965	345	Laurens	2	0	0
12-Sep-1965	2030	Avery	2	0	1
10-Dec-1966	330	Mecklenburg	2	0	0
2-May-1967	1910	Stephens	2	0	0
7-Jun-1968	1530	Greenville	2	0	0
18-Apr-1969	1745	Union, NC/Mecklenburg	2	0	0
18-May-1969	2200	Union, NC/Anson/Stanly	2	0	0
2-Apr-1970	640	Spartanburg	2	0	0
9-Apr-1970	1745	Hart	2	0	2
31-Mar-1973	1935	Franklin	2	0	0
31-Mar-1973	2000	Abbeville/Greenwood	4	7	30
24-May-1973	1520	Pickens/Greenville	2	0	0
27-May-1973	1920	York	2	0	2
27-May-1973	1930	Greenville/Spartanburg/Cherokee/Cleveland	3	0	49
27-May-1973	1930	Abbeville	2	0	7
27-May-1973	2300	Oconee	2	0	1
27-May-1973	2330	Pickens/Greenville	2	0	0
28-May-1973	1830	Oconee	2	0	0
21-Nov-1973	930	York	2	0	0
21-Nov-1973	1010	Stephens	2	0	0
13-Dec-1973	1453	Anderson	2	0	0
13-Dec-1973	1525	Greenwood/Laurens	2	0	3
13-Dec-1973	1545	Greenwood	3	0	26
2-Apr-1974	353	Greenwood	3	2	0
3-Apr-1974	2100	Graham/Swain	2	2	5
4-Apr-1974	900	Rabun	2	0	0
8-Apr-1974	1730	Caldwell	2	0	0
24-Mar-1975	1215	Anderson	2	0	0
24-Mar-1975	1315	York/Lancaster/Mecklenburg	2	0	5
18-May-1975	200	Union, NC/Anson/Stanly/Montgomery	2	0	1
14-May-1976	2215	Rutherford	2	0	0
23-Mar-1979	1630	Habersham	2	0	2
24-May-1979	1657	Greenville	2	0	2
13-Apr-1980	1850	Burke	2	0	0
13-Apr-1980	1910	Anderson	2	0	0
18-May-1980	240	Anderson/Greenville	2	0	5
23-May-1980	2110	Union, NC	2	0	0
6-Mar-1983	1920	Spartanburg	2	0	0
28-Mar-1984	1640	Union, NC	2	0	9
17-Aug-1985	1150	Laurens	2	0	43
4-Apr-1985	1609	Spartanburg	2	0	39
4-Apr-1985	1650	Oconee	2	0	0
4-Apr-1985	1718	Anderson/Greenville	2	0	0
4-Apr-1989	1530	Spartanburg	2	0	0
5-May-1989	1600	Habersham	2	0	3
5-May-1989	1720	Stephens	2	0	15
5-May-1989	1728	Spartanburg/Cherokee/Rutherford	4	2	35

5-May-1989	1754	Caldwell	2	0	0
5-May-1989	1901	Cleveland/Lincoln/Catawba	4	4	52
15-Nov-1989	1523	Union, NC	4	1	6
15-Nov-1989	1930	Greenwood	2	0	1
10-Feb-1990	900	Habersham	3	0	3
18-Oct-1990	1600	Cleveland	2	0	0
10-Mar-1992	2107	Union, NC	2	0	2
15-Apr-1993	1626	Mecklenburg	2	0	18
27-Mar-1994	1515	Union, SC	2	0	2
27-Mar-1994	1655	Oconee	3	0	12
16-Apr-1994	11	Spartanburg/Cherokee/Cleveland	2	0	2
26-Jun-1994	2330	Chester	2	1	4
16-Aug-1994	1450	Oconee	2	0	1
16-Aug-1994	1736	Union, SC/Spartanburg	3	0	0
16-Aug-1994	1805	Cherokee/Cleveland	2	0	0
16-Aug-1994	1845	Union, SC/Cherokee	2	0	1
16-Sep-1996	1540	Catawba	2	0	1
21-Feb-1997	1633	Anderson	2	0	2
7-Jan-1998	2110	Spartanburg	2	0	0
7-May-1998	1649	Pickens	2	0	4
7-May-1998	1655	Caldwell	4	0	2
7-May-1998	1749	McDowell	2	0	0
6-May-2003	1322	Lincoln	2	0	0
7-Sep-2004	1043	Elbert	2	0	12
16-Sep-2004	1450	York/Mecklenburg	2	0	0
16-Sep-2004	1645	Franklin	2	0	0
13-Jan-2005	1913	Franklin	2	1	1
14-Jan-2005	145	Laurens	2	0	1
7-Jul-2005	1210	Rowan	2	0	0
7-Jul-2005	1310	Alexander	2	0	0
15-Nov-2006	2345	Lincoln	2	0	0

Table 2. Mean and median values of sounding parameters associated with significant tornadoes across the western Carolinas and northeast Georgia. The third column contains values yielded by the composite soundings described in section 4. The values in the fourth and fifth columns are mean and median values from individual "ST day" soundings. The sixth column represents average values from Thompson at al. (2003, T03). *The 0-3 km CAPE value in the last column is from Rasmussen (2003), as T03 did not analyze this parameter.

Category	Parameter	Composite Value	Mean Value	Median Value	T03
Great Lakes (GRL)	0-6 km Shear (m s^{-1})	23	25	23	25
	0-1 km SRH (m^2 s^{-2})	124	125	103	165
	0-3 km SRH (m^2 s^{-2})	205	238	219	223
	sbCAPE (J kg^{-1})	827	1019	1030	2152
	0-3 km CAPE (J kg^{-1})	124	125	107	64*
	EHI	0.9	1.2	1.0	2.1
Ohio/Tenn Valley (OTV)	0-6 km Shear (m s^{-1})	25	26	28	24.5
	0-1 km SRH (m^2 s^{-2})	105	121	122	165
	0-3 km SRH (m^2 s^{-2})	206	238	255	223
	sbCAPE (J kg^{-1})	650	839	881	2152
	0-3 km CAPE (J kg^{-1})	71	99	92	64*
	EHI	0.7	1.2	1.2	2.1
Eastern Great Plains (EPL)	0-6 km Shear (m s^{-1})	24	25	27	24.5
	0-1 km SRH (m^2 s^{-2})	142	120	107	165
	0-3 km SRH (m^2 s^{-2})	231	222	172	223
	sbCAPE (J kg^{-1})	901	1348	1473	2152
	0-3 km CAPE (J kg^{-1})	57	84	72	64*
	EHI	1.2	1.7	1.7	2.1
Southeast Tropical Cyclone (TCY)	0-6 km Shear (m s^{-1})	14.1	16.1	16.7	24.5
	0-1 km SRH (m^2 s^{-2})	76	90	93	165
	0-3 km SRH (m^2 s^{-2})	141	142	147	223
	sbCAPE (J kg^{-1})	1150	1377	1284	2152
	0-3 km CAPE (J kg^{-1})	183	172	173	64*
	EHI	0.8	0.8	1	2.1
Outbreak	0-6 km Shear (m s^{-1})	23.8	24.9	23.9	24.5
	0-1 km SRH (m^2 s^{-2})	123	119	122	165
	0-3 km SRH (m^2 s^{-2})	240	246	244	223
	sbCAPE (J kg^{-1})	849	1101	1050	2152
	0-3 km CAPE (J kg^{-1})	93	109	99	64*
	EHI	1.2	1.5	1.4	2.1
All ST	0-6 km Shear (m s^{-1})	-	23.4	23.3	24.5
	0-1 km SRH (m^2 s^{-2})	-	106	95	165
	0-3 km SRH (m^2 s^{-2})	-	210	182	223
	sbCAPE (J kg^{-1})	-	1067	978	2152
	0-3 km CAPE (J kg^{-1})	-	117	108	64*
	EHI	-	1.1	1.0	2.1